

## 2. EXPLANATORY NOTES<sup>1</sup>

### Shipboard Scientific Party<sup>2</sup>

#### INTRODUCTION

This chapter describes the sampling, measurement, and core description procedures and methods used during Leg 153 to help the reader understand the basis for our preliminary conclusions and to help investigators select samples for further analysis. This chapter concerns only shipboard operations and analyses described in the site reports in the Leg 153 *Proceedings of the Ocean Drilling Program Initial Reports* volume. Methods used for shore-based analysis of Leg 153 data will be detailed in the *Scientific Results* volume.

#### Site Chapters

Descriptions of individual sites, operations summaries, and preliminary results are included in the site chapters. Detailed descriptions of each core sampled, thin-section descriptions, and photographs of each core follow the site chapter text. The separate sections in the site reports were written by the following shipboard personnel (listed in alphabetical order):

Principal Results: Cannat, Karson  
Operations: Cannat, Karson, Pettigrew  
Igneous Petrology: Barling, Casey, Fujibayashi, Kempton, Marchig, Miller, Niida, Ross, Stephens, Werner, Whitechurch  
Metamorphic Petrology: Cannat, Gaggero, Kelley, Whitechurch  
Structural Geology: Agar, Cannat, Ceuleneer, Dilek, Fletcher, Hurst, Karson  
Paleomagnetism: Gee, Hurst, Lawrence  
Physical Properties: Mutter  
Specialty Operations Tools: Holloway  
Summary and Conclusions: Cannat, Karson  
CD-ROM: Shipboard Scientific Party

Summary core descriptions (visual core descriptions for igneous and metamorphic rocks), thin-section descriptions, and photographs of each core follow the text of the site chapters.

#### Shipboard Scientific Procedures

##### Numbering of Sites, Holes, Cores, and Samples

Drilling sites are numbered consecutively from the first site drilled by DSDP's *Glomar Challenger* in 1968. A site refers to one or more holes drilled while the ship was positioned over a single acoustic beacon. Often multiple holes are drilled at a single site by pulling the drill pipe above the seafloor (out of the hole), offsetting the ship some distance from the previous hole (without deploying a new acoustic beacon), and drilling another hole.

For all ODP drill sites, a letter suffix distinguishes each hole drilled at a single site. The first hole at a given site is assigned the suffix A, the second hole is designated with the same site number and assigned

suffix B, and so on. Although this procedure differs from that used for DSDP Sites 1 through 624, it prevents ambiguity between site- and hole-number designations. The suffixes are assigned if penetration takes place, regardless of recovery. Distinguishing holes drilled at a site is important because recovered rocks from different holes, particularly when recovery is less than 100%, are likely to represent different intervals in the cored section.

The cored interval is measured in meters below seafloor; sub-bottom depths assigned to individual cores are determined by subtracting the drill-pipe measurement (DPM) water depth (the length of pipe from the rig floor to the seafloor) from the total DPM (from the rig floor to the bottom of the hole; Fig. 1). Water depths below sea level are determined by subtracting the height of the rig floor above sea level from the DPM water depth. The depth interval assigned to an individual core begins with the depth below the seafloor at which the coring operation began, and it extends to the depth at which the coring operation ended for that particular core (Fig. 1). Each coring interval is equal to the length of the joint of drill pipe added for that interval (~9.4–10.0 m). The pipe is measured as it is added to the drill string, and the cored interval is usually recorded as the length of the pipe joint to the nearest 0.1 m. However, coring intervals may be shorter and may not be adjacent if separated by intervals drilled but not cored or washed intervals.

Cores taken from a hole are numbered serially from the top of the hole downward. Core numbers and their associated cored intervals (in mbsf) usually are unique in a given hole; however, this may not be true if an interval must be cored twice because of caving of cuttings or other hole problems. The maximum full recovery for a single core is 9.5 m of rock contained in a core barrel (6.6 centimeter [cm] internal diameter) plus about 0.2 m in the core catcher (Fig. 2). The core catcher is a device at the bottom of the core barrel that prevents the core from sliding out when the barrel is being retrieved from the hole. Only rotary coring bits (RCBs) and steel and Cr-lined core barrels were used on Leg 153.

Cores are pulled from the core barrels and transferred into split, 1.5 m butylate core liners for curation and storage. The bottoms of oriented pieces (i.e., pieces that clearly could not have rotated about a horizontal axis in the core barrel) are marked with a red wax pencil to preserve orientation during the splitting and labeling process. Contiguous pieces with obvious features allowing realignment are considered to be a single piece. Plastic spacers are used to separate the pieces. Each piece is numbered sequentially from the top of each section, beginning with number 1; reconstructed groups of pieces are lettered consecutively (e.g., 1A, 1B, 1C, etc.; Fig. 3). Pieces are labeled only on external surfaces, and, if oriented, an "up" arrow is added to the label. Samples removed from the cores are designated by distance measured in centimeters from the top of the section to the top and bottom of each sample removed from that section. The spacers placed between pieces that do not fit together (for protection from damage during transit and storage) introduce void spaces between the pieces. Therefore, the centimeter interval noted for hard-rock samples has no direct relationship to that sample's depth in the cored interval.

Recovery rates are calculated based on the total length of a core recovered divided by the length of the cored interval (Fig. 1). As hard-rock coring operations are characterized by less than 100% recovery, the spacers between pieces can represent intervals of no recovery.

<sup>1</sup> Cannat, M., Karson, J.A., Miller, D.J., et al., 1995. *Proc. ODP, Init. Repts.*, 153; College Station, TX (Ocean Drilling Program).

<sup>2</sup> Shipboard Scientific Party is as given in the list of participants preceding the Table of Contents.

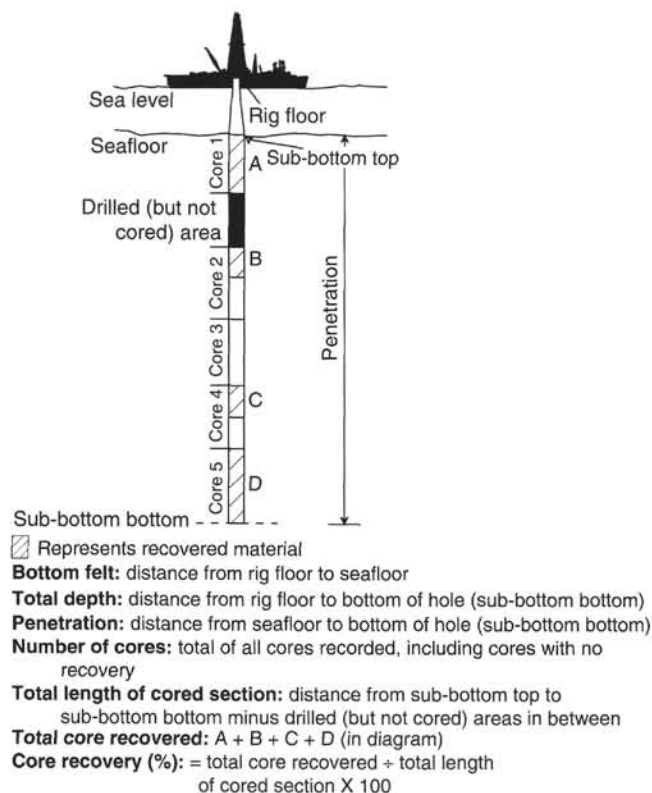


Figure 1. Diagram illustrating terms used in the discussion of coring operations and core recovery.

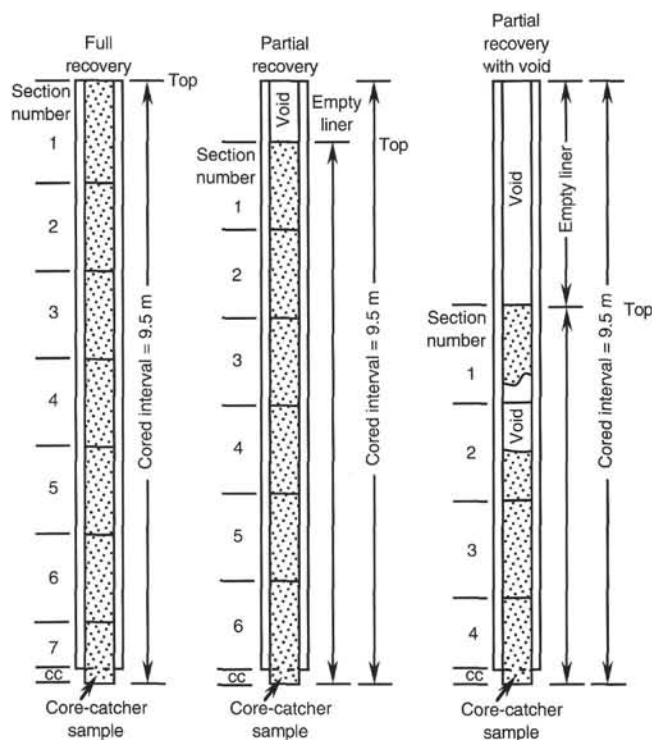


Figure 2. Diagram illustrating hard-rock core division.

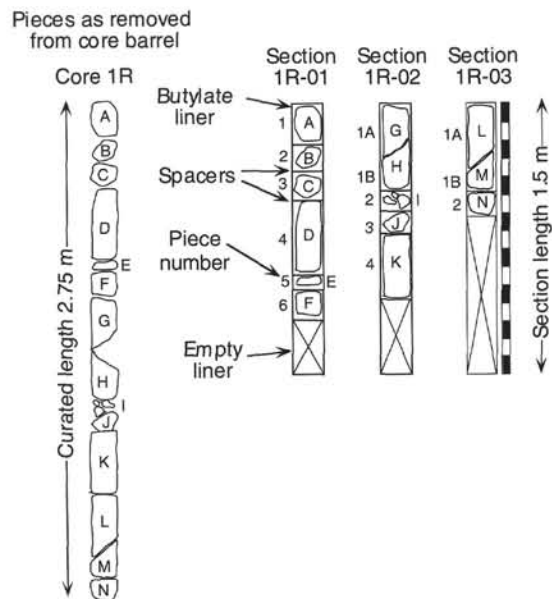


Figure 3. Core curation conventions for hard rocks. Letters designating pieces as removed from core barrel are for illustrative purposes only. Pieces A, B, C, D, E, and F become interval XXX-YYYZ-1R-01, Piece 1 to Piece 6 (where XXX is the leg, YYY is the site, and Z is the hole designator, respectively). Since Pieces G and H can be reoriented to fit along a fracture, they are curated as a single piece. In this case, the reassembled single piece is too long to fit in the bottom of Section 1R-01, so it is shunted to the top of Section 1R-02 and curated as interval XXX-YYYZ-1R-02 (Pieces 1A and 1B). Similarly, Pieces L and M are too long to fit in the bottom of Section 1R-02 after realignment and are shunted to the top of Section 1R-03. Spacers between pieces also artificially add length to the core when measured for archiving and curation. For example, Pieces L and M represent an interval from 2.17 to 2.63 m down from the top of the core as removed from the core barrel, but are archived as interval XXX-YYYZ-1R-03 (Pieces 1A and 1B, 0.0–46.0 cm).

ery up to the difference in length between a cored interval and the total core recovered. Most cores are designated "R" (rotary drilled) for curatorial purposes. In instances where coring intervals exceed the 9.5 m length of the core barrel, cores are curated as wash intervals and given the designator "W." When cores recovered from washed intervals are considered to be in situ, they are included in recovery rate calculations. The only other curation designator used on Leg 153 is "M" (miscellaneous), used to recognize cored material picked up in the bit or drill collar when the core barrel failed to engage.

## Core Handling

### Core Description

Continuous lengths of core longer than 20 cm are run through the multisensor track (MST) immediately after recovery. The MST includes the GRAPE (gamma-ray attenuation porosity evaluator and a magnetic susceptibility monitor). The core is then marked for splitting by a structural geologist who is charged with optimizing the appearance of structural features in the core while maintaining representation of any key features in both halves of the core and preserving the continuity of features that permeate more than one piece. The core is split with a diamond saw into archive and working halves. The archive half is photographed, and the pieces are measured and graphically represented on ODP forms (see "Archiving," this chapter). Most archive sections more than 20 cm long are run through the cryogenic magnetometer. Close-up photographs (black-and-white) used for illustration of key features in the summary of each site are taken at the request of the shipboard scientific party. Because the core was in transit prior to

the Leg 153 post-cruise meeting and not available for examination, color close-up photographs of selected parts of the core were taken.

After the cores are described and the data archived, the working halves are sampled for shipboard thin-section, physical properties, paleomagnetic, and chemical analyses. All samples were curated, sealed in containers, and labeled. Records of all samples are kept by the curator at ODP.

Both halves of the core are shrink-wrapped in plastic to prevent damage or movement during shipping and are put into labeled plastic tubes, sealed, and transferred to cold storage facilities aboard the drilling vessel. All Leg 153 cores are housed in the Bremen Core Repository (BCR) in the Federal Republic of Germany.

### Archiving

For archiving core descriptions on Leg 153, the modified visual core description (VCD) forms developed on ODP Leg 147 (Shipboard Scientific Party, 1993) were used. These forms summarize the igneous, metamorphic, and structural features of the core, and present a graphical representation of the pieces recovered (Fig. 4). The left column of the form is a graphic representation of the archive half of the core. A horizontal line across the entire width of the column represents the plastic spacer glued between rock pieces in the core liner. Oriented pieces are designated with an arrow in the column labeled "Orientation." Shipboard samples and studies are indicated on the VCD form with the following notation: XRF = X-ray fluorescence analysis; XRD = X-ray diffraction analysis; TS = polished petrographic thin section; PM = paleomagnetic analysis; and PP = physical properties analysis. Lithologic units are defined according to the method outlined in "Igneous Petrology," this chapter. Igneous lithologies are represented by a series of patterns defined in Figure 5. Symbols used to note metamorphic intensity and structural features are also presented in Figure 5 and defined in the "Metamorphic Petrology" and "Structural Geology" sections (this chapter).

Data from these forms are entered into the shipboard computerized archiving system (ROCKY) and are available from the ODP data librarian. For each lithologic unit and section the following data are recorded in the ROCKY archiving system:

- A. Leg, site, hole, core number, core type, and section number.
- B. Unit number (consecutive downhole), piece numbers of the same lithologic unit, rock name, and identification of the observer.
- C. Color of the dry rock.
- D. Mineral phases visible with a hand lens or binocular microscope, their distribution, and the following information for each phase: abundance (vol%), size range (mm), habit (anhedral, subhedral, or euhedral), degree of alteration (%), and other comments.
- E. Texture of the rock defined by absolute grain size: glassy, fine-grained (<1 mm), medium-grained (1–5 mm), coarse-grained (5–30 mm), and very coarse-grained (>30 mm). Grain-size variability within a lithologic unit is also recorded, as is relative grain size (equigranular or inequigranular).
- F. Abundance, distribution, size, and shape of any voids (vesicles, miairoles, cavities, etc.).
- G. Presence and characteristics of any secondary minerals, including mode of occurrence (void-filling or replacive), association with primary minerals, depositional sequences, overprinting relations, and relationship to rock fabric.
- H. Intensity of metamorphism, expressed as the percentage of primary phases replaced by secondary phases: negligibly metamorphosed (<2%), slightly metamorphosed (2%–10%), moderately metamorphosed (10%–40%), highly metamorphosed (40%–80%), and pervasively metamorphosed (>80%).
- I. Presence of veins and fractures, including abundance, width, filling or coating, orientation, crosscutting relationships, and presence of alteration halos within the adjacent rock.
- J. Presence of structural features including the type (sharp, gradational, faulted, missing), orientation, nature (sutured igneous, intru-

sive, crosscutting), aspect (chilled up, down, or sideways, grain size, modal), and morphology (planar, irregular) of igneous contacts, igneous layering, magmatic fabric (igneous foliation, etc.), crystal-plastic fabric, cataclastic features, fractures and faults, and veins.

K. Other comments, including notes on the continuity of the unit within the core and on interrelationship of units.

All thin sections taken aboard ship are fully described in terms of igneous, metamorphic, and structural character in order to complement and refine the macroscopic descriptions recorded from core observation. These petrographic descriptions are archived in ROCKY and are used to help define unit boundaries based on mineral assemblages, and to examine microstructural and fabric features. All thin sections prepared for shipboard study are polished petrographic sections without cover slips. Thin-section billets are selected by the scientific party to be representative of major lithologies, and additional thin sections are prepared as requested by specific scientists and as time allows. For each thin section, the following information is recorded:

- A. Leg, site, hole, core number, core type, section number, piece number, and centimeter interval of sample.
- B. Unit number (consecutive downhole), rock name, and identification of the observer.
- C. Grain size, using the same terminology defined for VCD.
- D. Texture, including terms describing crystallinity, fabric, and crystal interrelationship.
- E. Primary mineralogy; for fine-grained rocks this is divided into phenocrysts and groundmass, for coarse-grained rocks the division is major and accessory mineralogy, including either point-counted modal abundance where number of points and stepping interval from an automatically advancing stage are noted, or visually estimated modal abundance noting percent of phase present, percent of phase originally present, size (mm), composition, habit, and additional description and comments.
- F. Secondary mineralogy, including percent present, replacing/infilling, size (mm), habit, and additional description and comments.
- G. Cavities, including type, present and original percent, size (mm), shape, infilling, and additional description and comments.
- H. Structures, primary and secondary features including foliation, lineation, contacts, and deformation (type and degree).
- I. Veins and fractures, including descriptions of infilling, crosscutting, orientation, alteration halos, etc.
- J. Additional comments.

## IGNEOUS PETROLOGY

Observations on hard rock petrology and petrography were stored both in ODP written and electronic media and in project-designed Microsoft Excel spreadsheet files according to definitions below and the terminology and outlines described in "Linked Spreadsheets and Database" (this chapter). For detailed discussions of hard-rock core "barrel sheets," refer to the "Igneous Petrology" sections in the "Explanatory Notes" in *Initial Results* volumes for Legs 145 and 147. Hand-sample mesoscopic to microscopic observations on igneous and mantle-derived ultramafic rock core were recorded in the VCD Microsoft Excel spreadsheet by the igneous petrologists. Microscopic descriptions on standard petrographic thin sections were recorded in the TSPERID spreadsheet for peridotites and the TSGAB spreadsheet for gabbroic rocks. The types of data entered into these files are defined below. These spreadsheets are recorded on the Leg 153 CD-ROM (back pocket, this volume).

### Rock Classification

Igneous rocks were classified on the basis of grain size, texture, and the abundance of primary minerals. Mafic aphanitic volcanic rocks were described as glassy, aphyric, or phyrlic. Volcanic rocks were

## UNIT 13: SERPENTINIZED HARZBURGITE

## Pieces 1–17

**COLOR:** Dark gray.**PRIMARY STRUCTURE:** Porphyroclastic.**PRIMARY MINERALOGY:**

Olivine - Mode: 90%–95%.

Orthopyroxene - Mode: 5%–10%.

Crystal Size: 1–10 mm.

Crystal Shape: Anhedral.

Crystal orientation: Tectonic.

Spinel - Mode: &lt;1%.

Crystal Size: &lt;2 mm.

Crystal Shape: Anhedral.

Comments: The rock comprises serpentized weakly porphyroclastic harzburgite cut by numerous 10–50 mm gabbroic to pyroxenitic veins (now strongly altered). Orthopyroxene abundance is consistently around 8%–12%, and clinopyroxene is absent or accessory, except as associated with veins. Metagabbro/pyroxenite veins are developed in Pieces 1, 4, 6, and 10, while thinner tremolite-rich veins along zones of pyroxene recrystallization/growth are present in Pieces 1, 3, 13, 15, and 17. Piece 1 contains five altered pyroxenite/gabbro composite veins that range in orientation from parallel to highly oblique to the foliation plane defined by the preferred dimensional orientation of orthopyroxene porphyroclasts. Piece 2 is harzburgite rubble with pyroxenite vein material. Piece 3 contains a strongly altered pyroxenite vein 4 cm thick. Piece 4 contains a strongly altered 2.5 cm thick branching and highly altered gabbroic vein. Pieces 6 and 10 are composed of thick (>4 cm thick) composite pyroxenite/gabbro veins that are highly altered. In general, there is a high density of vein material in the section and this is correlated with generally low total pyroxene content in the harzburgite.

**SECONDARY MINERALOGY:**

Serpentine.

Total Percent: 95

Comments: Replaces primary phases.

Magnetite.

Total Percent: &lt;1

Comments: Product of serpentinization.

Comments: Harzburgite in this section is variably altered. Pieces 1 and 3 are less than 70% altered. In Piece 3, this less altered interval occurs near a metagabbro/pyroxenite vein now replaced by amphibole and chlorite. In the other pieces, alteration is 90%–98%. Olivine is 70%–99% altered to a gray, dark gray serpentine and iron oxide mineral-rich mesh. Talc may be present near altered magmatic veins. Pyroxene is 60%–95% serpentinized, and marginally replaced by amphibole, chlorite, and talc, also near the altered magmatic veins. The gabbroic and pyroxenitic veins (up to 50 mm wide, Pieces 1, 4, 6, and 10) are characterized by early brown amphibole replaced by actinolite, epidote, chlorite, and late zeolite. They typically show chloritic rims. Late serpentine and sulfide mineral veins cut the metagabbro. Veins, and coarse impregnations along fractures, of clinopyroxenite are altered to actinolite/tremolite in Pieces 1, 2, 3, 13, 15, and 17. These veins are typically <1 to 10 mm in width. Later serpentine-bearing veins (2–4 mm wide) are found in Pieces 10 and 11. Thin white to pale green discontinuous serpentine veins occur in most pieces. This section lacks development of anastomosing wispy serpentine vein networks.

**VEIN/FRACTURE FILLING:**

Metagabbro (brown amphibole, actinolite, chlorite, and zeolite?).

Size: 10–50 mm.

Serpentine and pyrite.

Size: &lt;2 mm.

Orientation: Crosscutting.

**ADDITIONAL COMMENTS:** Structure

A moderately elongated porphyroclastic fabric is present in the upper part of the section, particularly Piece 1. This fabric diminishes in the lower part of the section. No orientation could be measured for the foliation. Metagabbro veins and altered clinopyroxenite veins commonly display bifurcating branches and show no preferred orientation (e.g., Pieces 4 and 15). In Piece 15 an altered clinopyroxenite is cut by a thin, white serpentine vein that parallels the foliation. In Piece 4, a pale green serpentine vein cuts across a metagabbro vein.

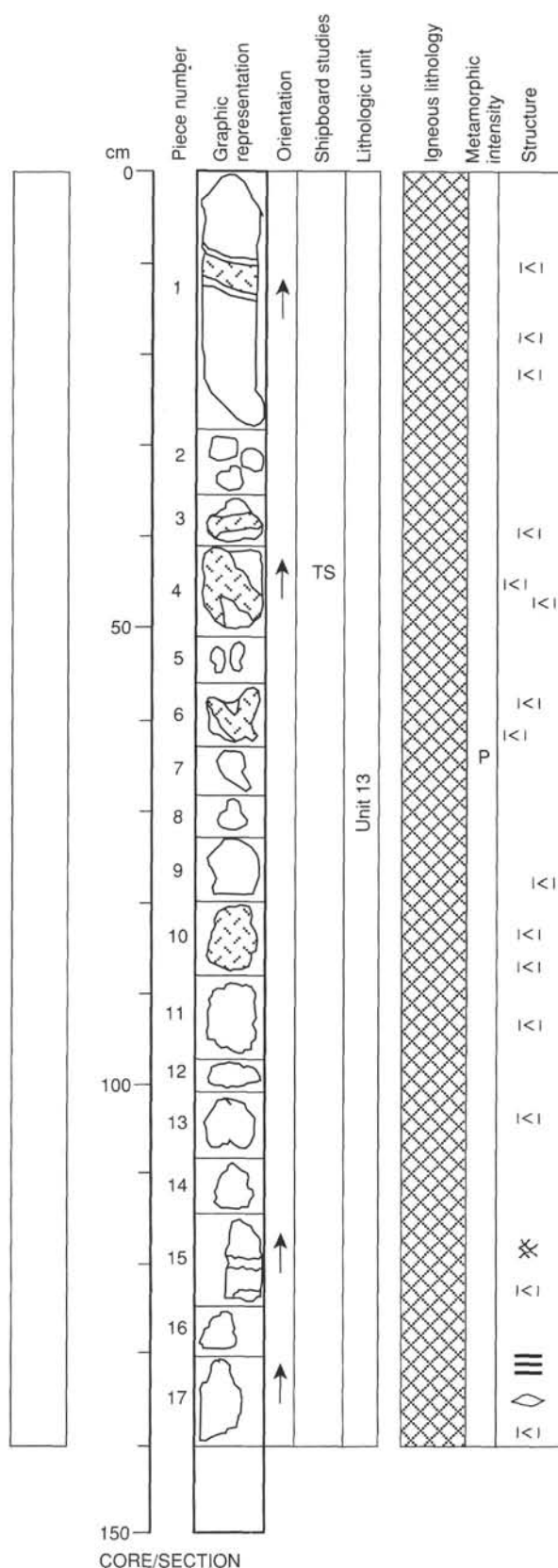


Figure 4. Example of the visual core description form used during Leg 153.



defined as aphyric if phenocryst abundances were <1%, sparsely phyrical between 1% and 2%, moderately phyrical between 2% and 10%, or highly phyrical >10%. Phenocryst abundances were recorded as visually estimated percentages and modal estimates of thin sections.

Mafic, ultramafic, and silicic phaneritic rocks were classified according to Streckeisen (1974) as shown in Figure 6. In the case of ultramafic rocks, the term "primary assemblage" was used to refer to the estimated pre-hydration mineral assemblage. Most of the ultramafic rocks sampled were interpreted to be mantle rocks that experienced high-temperature, dynamic metamorphic recrystallization during upwelling and melting in the mantle, followed by a second stage of lower temperature static replacement and/or dynamic recrystallization during their emplacement near the seafloor under lower temperature, hydrous conditions. Rock names were assigned based on the primary phases that existed prior to hydration and serpentinization. Where hydrous alteration in ultramafic rocks was so extensive that estimation of the primary phase assemblages was not possible, the rock was called "serpentinized." If primary assemblages, their pseudomorphs, and textures could still be recognized in ultramafic samples, even though they were partially or completely serpentinized and altered, the rock name was based on the reconstructed primary assemblage, and the adjective "serpentinized" was added (e.g., serpentinized dunite, serpentinized harzburgite, serpentinized lherzolite). When secondary hydrous minerals exceed 50 modal% in mafic plutonic rocks, the prefix meta- was used with the igneous protolith name where possible (see "Metamorphic Petrology," this chapter). If the mafic rock exhibits the effects of dynamic metamorphism such that the assemblages consist of secondary hydrous minerals that completely obliterate the protolith texture or is made up of recrystallized primary minerals, the appropriate metamorphic rock names were used. The textural terms "mylonitic," "schistose" and "gneissic" (see "Structural Geology," this chapter) were added to metamorphic rock names, such as "amphibolite" or "metagabbro" to indicate that the rocks exhibit the effects of dynamic metamorphism.

For gabbroic rocks, the qualifiers mela- or leuco- were used to indicate samples that contain either high proportions (>65%) of mafic minerals or plagioclase, respectively, as shown in Figure 6. The presence of additional mineral phases was indicated by a mineral name qualifier (e.g., oxide gabbro) where the abundance of that mineral exceeds 5% of the mode and very coarse grain sizes (in excess of 3 cm) were indicated by the qualifier "pegmatitic" preceding the rock name.

### Primary Silicate Minerals

The principal rock-forming minerals in the core recovered are plagioclase, olivine, clinopyroxene, and orthopyroxene. For each of these minerals, the following data were recorded in the VCD log and ROCKY: (1) estimated modal percent of the primary and secondary minerals; (2) smallest and largest size of mineral grains (measured along the longest axis in mm); (3) crystal shape using the terms euhedral, subhedral, and anhedral; and (4) three-dimensional crystal shape using standard terms such as equant, tabular, platy, etc. (see terminology spreadsheet and "Linked Spreadsheets and Database" section, this chapter). In addition, accessory phases such as spinel, other oxide minerals, and sulfide minerals were also noted. Also listed were the percentage alteration of each primary phase, the alteration minerals, and the total alteration for the rock. In general, these descriptions and estimates were conducted by hand sample inspection, except for a more limited sample suite for which point counted or visual modal estimates were available from thin sections.

### Igneous Textures

Crystallinity, granularity (the absolute and the relative sizes of crystals), crystal shapes, and arrangement of crystals were recorded as the main properties of texture (McKenzie et al., 1982). The absolute ranges of grain size in the rocks were recorded for each primary

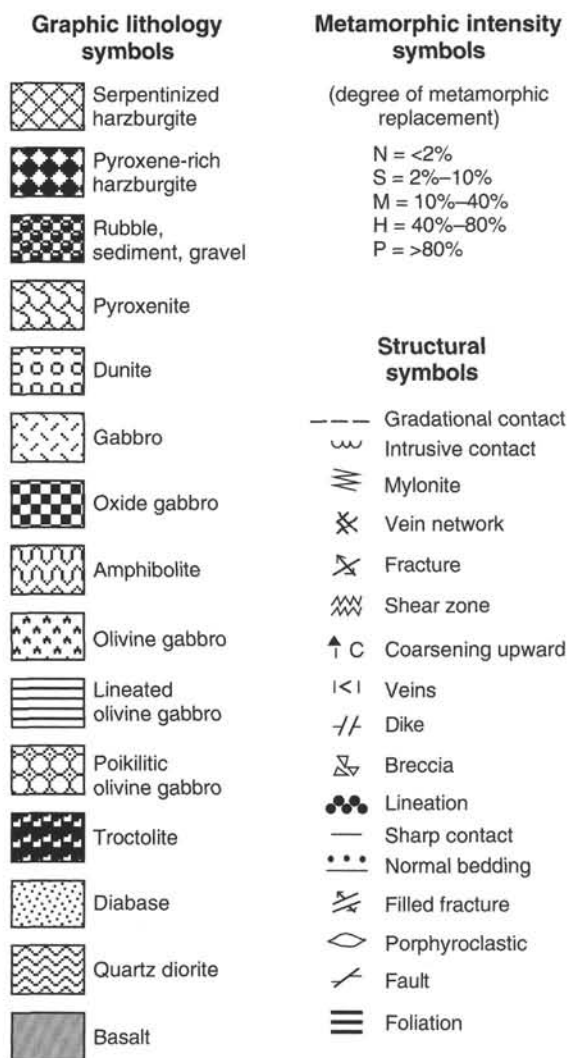


Figure 5. Legend for visual core description forms.

phase in each piece of the core described. These ranges were recorded in VCD, TSPERID, and TSGAB. The terms coarse-grained (crystal diameters 5–30 mm), medium-grained (crystal diameters 1–5 mm), and fine-grained (crystal diameters <1 mm) were applied based on these data and adopted for reporting purposes and summary notes. If the grain size exceeded 30 mm, the rock was described as pegmatitic.

The rocks were further subdivided on the basis of relative grain size into equigranular and inequigranular rocks. The equigranular rocks were described as follows: (1) panidiomorphic granular (the bulk of the crystals are euhedral and of uniform size); (2) hypidiomorphic granular (the bulk of the crystals are subhedral and of uniform size); and (3) allotriomorphic granular (the bulk of the crystals are anhedral and of uniform size). Inequigranular rocks were described in the following manner:

1. Seriate (the crystals of the principal minerals show a continuous range of sizes).
2. Poikilitic (relatively large crystals of one mineral [oikocryst] enclose numerous smaller crystals of one or more other minerals [chadacrysts]).
3. Ophitic/subophitic (a variation on poikilitic texture in which the randomly arranged bladed crystals, usually of plagioclase, are wholly or partly enclosed by the oikocrysts usually of pyroxene).
4. Intergranular (spaces between plagioclase laths are occupied by one or more grains of pyroxene, olivine, and opaque minerals).

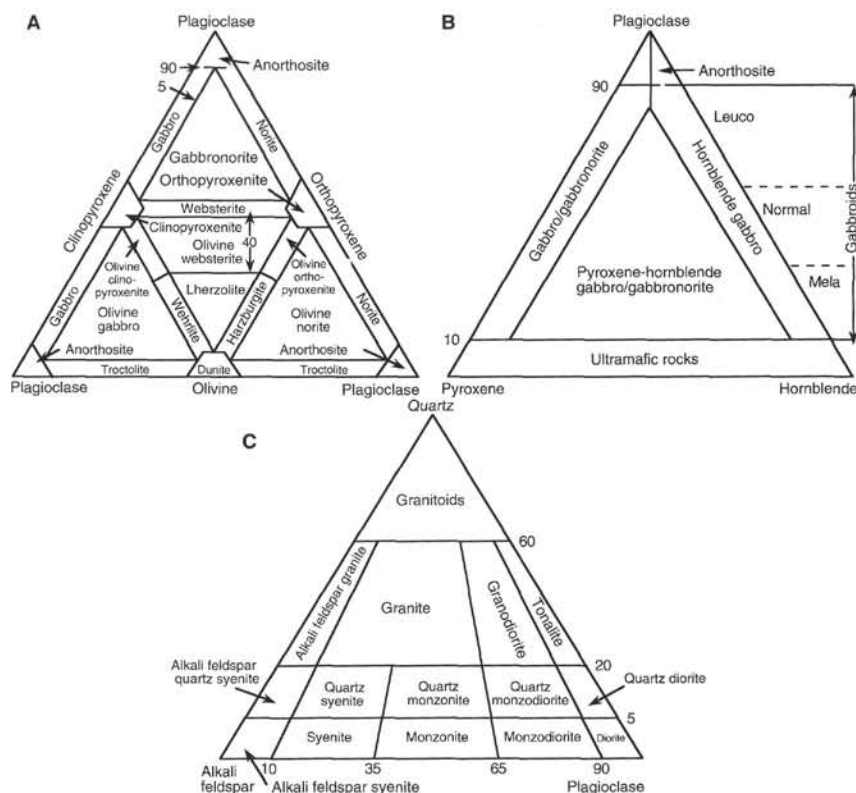


Figure 6. **A.** Classification of ultramafic and gabbroic rocks composed of olivine, clinopyroxene, orthopyroxene, and plagioclase (after Streckeisen, 1974). **B.** Classification of gabbroic rocks composed of plagioclase, hornblende, and pyroxene (Streckeisen, 1974). **C.** Classification of silicic plutonic rocks composed of quartz, plagioclase, and alkali feldspar (Streckeisen, 1974).

5. Porphyritic (relatively large crystals are surrounded by finer-grained groundmass; basalt and diabase with this texture were recorded as mildly, moderately, and strongly phytic); and

6. Glomeroporphyritic (a porphyritic texture where the phenocrysts are clustered in aggregates). If there was a marked random change in texture within a lithologic unit, it was described as varitextured.

### Igneous Structure

In plutonic rocks, igneous structures can be especially important in defining the mechanism of crystallization of the primary mineralogy. Igneous fabric for each primary phase was recorded in the VCD, TSPERID, and TSGAB logs and later recorded in the ROCKY database. Terms used include homogeneous (or unstructured), varitextured where an abrupt and random variation in texture occurs (ranging from coarse or pegmatitic to very fine-grained), layered where distinct sheet-like cumulate units exist, and laminated where thin (<1.0 cm), sharply defined units occur. Visibly graded layers were defined by (1) modal variation in the primary mineralogy, (2) grain-size variation, or (3) textural variation (e.g., from poikilitic to granular). The sense of grading was related to the position of the top of the core, except where layering is vertical. Normal grading was recognized as either from coarse to fine grain size or from dark to light mineralogy upward in a layer. Reverse grading was considered the opposite. Where a crystal alignment of probable igneous origin was observed, this was recorded as shape preferred dimensional orientation and measured by the structural geologists. The internal structure, contacts, and the thickness of the layering, and the orientations of any planar or linear structures were recorded on the structural VCD Spreadsheet (see "Structural Geology," this chapter).

### Thin-Section Description

Thin sections of igneous rocks were examined to complement and refine the hand-specimen observations. In general, the same type of data were collected from thin sections as from visual descriptions, and a similar terminology was used. Modal data were also collected from

representative thin sections using standard point-counting techniques. Visual estimates were made on all the remaining thin sections. All data were recorded in the ROCKY and the thin-section spreadsheets (TSPERID and TSGAB). Because volume expansion during serpentinization causes an increase in area on any plane within an ultramafic rock, serpentine counted in thin sections as olivine will tend to exaggerate the olivine mode in the sample. Accurate reconstruction of peridotite primary assemblages modes were not possible aboard ship because these reconstructions require additional information such as the bulk-rock and mineral chemistry data on each sample. Therefore we have reported only the abundance of serpentine after olivine and pyroxene.

Some additional textural features were recorded. Aphanitic rocks were distinguished either as microcrystalline (crystals identified in thin section with a petrographic microscope) or as cryptocrystalline (crystals too small to be identified with a microscope). Crystal sizes were measured using a micrometer scale and are generally more precise than visual estimates. The presence of inclusions, overgrowths, and zonation was noted, and the apparent order of crystallization was suggested in the comment section for samples with appropriate textural relationships. The presence of accessory minerals such as apatite, zircon, oxide minerals, and sulfide minerals was noted. The percentage of alteration minerals and hydrothermal sulfide minerals were also reported (see "Metamorphic Petrology," this chapter).

Where thin-section inspection or visual rock descriptions allowed preliminary interpretations of cumulate textures (orthocumulate, mesocumulate, adcumulate, heteradcumulate, and crescumulate), they were entered into the VCD and thin-section sheets. In practice these descriptions were made during thin-section inspection by estimation of the proportion of cumulus minerals and the interstitial minerals solidified in pore spaces between them. Use of these "cumulate" terms does not imply that these rocks formed as a result of crystal settling (as redefined in Irvine, 1981), but rather they are used practically and descriptively to express the relative abundance and nature of post-cumulus and cumulus (or primocryst) phases (and not in the more genetic sense as originally proposed by Wager et al., 1960). For the purposes of this study, a "cumulate" is then defined as an igneous rock characterized by a framework of mineral (cumulus) crystals that were

Table 1. X-ray fluorescence (XRF) operating conditions, analytical error estimates, and detection limits.

Oxide or element	Line	Crystal	Detector	Collimator	Peak angle (°2 $\theta$ )	Background offset (°2 $\theta$ )	Count time on peak (s)	Count time on background (s)	Analytical error (rel. %)	Detection limit
SiO <sub>2</sub>	K-alpha	PET	FPC	Medium	109.21		40		0.30	0.03
TiO <sub>2</sub>	K-alpha	LIF200	FPC	Fine	86.14		40		0.37	0.01
Al <sub>2</sub> O <sub>3</sub>	K-alpha	PET	FPC	Medium	145.12		100		0.40	0.01
Fe <sub>2</sub> O <sub>3</sub>	K-alpha	LIF200	FPC	Fine	57.52		40		0.20	0.01
MnO	K-alpha	LIF200	FPC	Fine	62.97		100		0.10	0.005
MgO	K-alpha	TLAP	FPC	Medium	45.17	±0.80	150	150	0.60	0.01
CaO	K-alpha	LIF200	FPC	Medium	113.09		40		0.30	0.005
Na <sub>2</sub> O	K-alpha	TLAP	FPC	Medium	54.10	-1.20	150	150	3.80	0.03
K <sub>2</sub> O	K-alpha	LIF200	FPC	Medium	136.69		100		0.40	0.01
P <sub>2</sub> O <sub>5</sub>	K-alpha	GE111	FPC	Medium	141.04		100		0.40	0.01
Rh	K-alpha Compton	LIF200	Scint	Fine	18.58		60			
Nb	K-alpha	LIF200	Scint	Fine	21.40	+0.35	200	100	0.2	0.5
Zr	K-alpha	LIF200	Scint	Fine	22.55	-0.35	100	50	0.5	0.6
Y	K-alpha	LIF200	Scint	Fine	23.80	-0.40	100	50	1.0	0.6
Sr	K-alpha	LIF200	Scint	Fine	25.15	-0.40	100	50	0.3	0.6
Rb	K-alpha	LIF200	Scint	Fine	26.62	-0.60	100	50	3.6	0.6
Zn	K-alpha	LIF200	Scint	Medium	41.81	-0.55	100	50	1.0	1.0
Cu	K-alpha	LIF200	Scint	Fine	45.03	-0.55	100	50	1.5	1.2
Ni	K-alpha	LIF200	Scint	Medium	48.67	-0.60	100	50	0.6	1.2
Cr	K-alpha	LIF200	FPC	Fine	69.35	-0.50	100	50	1.3	2.0
V	K-alpha	LIF200	FPC	Fine	123.06	-0.50	100	50	2.0	3.0
Ti	K-alpha	LIF200	FPC	Fine	86.14	+0.50	40	20		
Ce	L-alpha	LIF220	FPC	Medium	128.13	-1.50	100	50		
Ba	L-beta	LIF220	FPC	Medium	128.78	-1.50	100	50		

Notes: All major elements measured using a rhodium X-ray tube operated at 30 kV and 80 mA. Trace elements are measured using a rhodium X-ray tube operated at 60kV and 50mA. Detector: FPC = flow proportional counter (P10 gas); Scint = NaI Scintillation counter. Detection limits in wt% for major oxides, ppm for trace elements.

concentrated primarily through fractional crystallization of a magma. The exact mechanism of concentration (flotation, settling, in-situ crystallization) need not be specified. Their bulk composition is generally unlike known magma types. The cumulate textural classification is simply an attempt to distinguish between two different stages of solidification of plutonic rocks, that of cumulus minerals and that of intercumulus liquid (postcumulus minerals). A similar attempt is commonly made in finer grained rocks such as highly porphyritic diabase or basalt, except that the cumulus minerals are a smaller fraction of the rock and grain-size distinctions provide a clearer view of the two stages of solidification.

As described by Irvine (1981), in an orthocumulate the post-cumulus materials should be abundant (and mostly interstitial) and the cumulus phases should ideally exhibit much of their original crystallization forms with rims of variable widths that are strongly and normally zoned (especially in the case of plagioclase, which does not re-equilibrate as readily as mafic phases). Postcumulus minerals generally make up ≈25%–50% of the rock in orthocumulates. Mesocumulates have less postcumulus material (≈7%–25%), and the cumulus grains should join along mutual interference boundaries developed through overgrowth. Adcumulates have only minor discrete post-cumulus material (≈0%–7%), and mutual interference boundaries developed through overgrowth. A variant on adcumulate is heteradcumulate, usually described in poikilitic rocks in which unzoned oikocrysts, believed to have grown through adcumulus processes, engulf and enclose primocrysts (chadacrysts). Crescumulate texture is reserved for plutonic rocks with dendritic crystal forms that are oriented with their long axes perpendicular to layering and are thought to result from in-situ crystallization.

It is also important to recognize that rocks are likely to be affected by post-cumulus metasomatic and replacement processes in addition to static overgrowths caused by crystallization of the cumulus pore melt either trapped or in communication with the magma reservoir. A critical evaluation of the relative abundance and nature of post-cumulus material awaits detailed shore-based textural, mineral, and bulk rock geochemical studies to assess whether final solidification was associated with trapped or migrant pore melts.

## Geochemistry

Samples considered by the shipboard scientific party to be representative of the various lithologies cored were analyzed for major oxide and selected trace element compositions by X-ray fluorescence. Details of the shipboard analytical facilities and methods are presented in previous ODP *Initial Reports* volumes (e.g., Volumes 118, 140, and 147). A list of the elements analyzed and the operating conditions for Leg 153 XRF analyses appear in Table 1.

Chemical analyses on ultramafic and gabbroic rocks were performed as described in the "Explanatory Notes" of the Volume 147 *Initial Reports*, with a few exceptions as outlined below. After coarse crushing, samples were ground in a tungsten carbide shatterbox. The high bound-water content of the serpentinized peridotites sampled at Site 920 caused excessive clumping of the powders during grinding. This problem was overcome by adding a small amount of chemical grade acetone to the shatterbox prior to grinding.

Loss on ignition (LOI) for each sample was determined by the standard practice of heating an oven-dried (110°C) sample to 1010°C for several hours. In order to more fully investigate the results of LOI determinations, gas chromatography of the expelled volatiles was performed on a Carlo Erba NA 1500 CHS analyzer. Five to 10 mg of dried (110°C) rock samples were combusted at 1010°C, releasing water and carbon dioxide. During this process, sulfur from sulfide minerals is oxidized to SO<sub>2</sub> (by addition of V<sub>2</sub>O<sub>5</sub>), and SO<sub>3</sub> is released from any sulfate minerals present in the sample. Gas-chromatographic separation was followed by quantitative determination of the respective gaseous oxides of carbon, hydrogen, and sulfur by a thermal conductivity detector. The NBS standard NBS 1646 Estuarine Sediment (6.37% CO<sub>2</sub> and 6.12% H<sub>2</sub>O) and the shipboard diabase standard BAS 140 (Dick, Erzinger, Stokking, et al., 1992) were used to calculate the bias factor of the CHS analyzer and to test accuracy and reproducibility of the method. Sulfur concentrations were below the detection limit of 200 ppm. Higher sample weights might have increased the accuracy of sulfur determinations, but they would likely have resulted in incomplete combustion and accumulation of debris in the combustion tube.



In order to overcome the effects of high concentrations of bound water present in the serpentinized peridotite samples on trace element compositions, these compositions were measured on pressed pellets prepared from ignited powders. This approach was undertaken to permit comparisons with anhydrous peridotites.

### Igneous Lithology, Unit Definition, and Summary

For a complex sequence of plutonic rocks, interpretations of the vertical lithologic successions in the core are difficult because of overprinting of syn-magmatic metamorphic and tectonic processes. The lithologic units adopted here were defined by vertical sections with consistent internal characteristics and lithology and are separated based on geological contacts defined by significant changes in modal mineralogy or texture, as encountered downhole. Both sharp and gradational unit contacts occur in these types of rocks on the scale of the core. If the contact was recovered, its location was recorded by the core, section, position (in centimeters [cm]), piece number, and unit number. When the contact was not recovered, but a significant change in lithology or texture was observed, the contact was placed at the lowest piece of a unit. The information recorded for each section of the core includes the rock type, igneous, metamorphic, and/or deformational texture, evidence for igneous layering, extent, type and intensity of deformation, primary and secondary minerals present, grain shape for each primary mineral phase, evidence of preferred orientation, the percent alteration of the primary phases, contact relationships, small magmatic veins, secondary mineral veins, and general comments. These rock descriptions in the VCD log formed the basis for dividing the core into basic lithologic units. The description and summary of each unit was entered into the ROCKY database where the general lithological description and top and bottom of the unit were recorded with reference to curated core, section, piece(s), depth, and thickness. Also included in ROCKY are summary notes on textural variations, primary, accessory, and alteration phases, structural information, and the contact relationships for each unit derived from the more detailed data recorded in VCD, TSPERID, and TSGAB. Parts of the hole drilled but not cored and mixed lithology rubble recovered after reaming and washing the hole were included in the tabulation, but were not considered lithologic units.

### METAMORPHIC PETROLOGY

Visual core descriptions of metamorphic characteristics were conducted together with igneous and structural documentation of the core. This information was recorded to provide two types of data: (1) the extent of replacement of igneous minerals by metamorphic, or secondary minerals; and (2) the extent to which metamorphic minerals contribute to any subsolidus fabric found in the core. The relative timing of metamorphic crystallization and deformation, and the overprinting relationships between secondary minerals were reported in the comments of the ROCKY database. To ensure accurate core descriptions, thin-section petrography of representative samples was integrated with visual core descriptions. Identification of mineral phases was checked by XRD analyses according to ODP standard procedures outlined in previous *Initial Reports* volumes (e.g., Volume 118). For each core section, the following information was recorded: the leg, site, hole, core number, core type, section number, piece number (consecutive downhole), and position in the section.

#### Macroscopic Description

The metamorphic mineral assemblages were recorded in the ROCKY database. Primary phases and the secondary minerals that replace them were noted, and the volume percent of each phase was estimated in hand specimen and checked by modal analyses of thin sections. Portions of pieces where primary textures were ambiguous or

obliterated by secondary minerals were termed "patches" and their mineralogy was recorded in the ROCKY database. The term rodingite was used for metasomatized mafic rocks associated with serpentinites that are characterized by incipient "Ca-metasomatism," the pervasive replacement of plagioclase by hydrogrossular, prehnite, and/or epidote, and the destruction of igneous textural relationships.

Alteration intensity was classified as follows: negligible (<2%), slight (2%–10%), moderate (10%–40%), high (40%–80%), and pervasive (80%–100%). A column in the (VCD) spreadsheet (Fig. 7) shows the variation in alteration intensity in the core. Electronic versions of these spreadsheets reside in the "SPREADS" folder of this volume's accompanying CD-ROM (back pocket).

### Description of Metamorphic Fabric

Where metamorphic minerals are included in fabric elements such as shear zones, mylonites, or foliations, textures and associated minerals were recorded in the ROCKY database. For samples affected by crystal-plastic deformation, textural features noted included identities and abundance (in volume percent) of porphyroclasts and their alteration products, of neoblasts, and of other minerals associated with and defining the fabric. Metamorphic textures recorded included classification of cataclastic, mylonitic, schistose, and gneissic features.

Metamorphic facies names such as amphibolite, greenschist, and zeolite were applied according to the general definitions of Best (1982) and Yardley (1989), excepting the use of the term "granulite facies." In general, the mineral assemblage of this facies has been defined on the basis of continental rocks that typically contain augite + orthopyroxene + Ca plagioclase + Mg-Fe garnet. Because geothermal gradients and rock compositions are significantly different at mid-ocean ridges when compared with their continental counterparts, oceanic granulite assemblages are unlikely to be mineralogically similar to continental granulites that typically form under higher pressure conditions. In a mid-ocean ridge environment, dynamically recrystallized gabbroic rocks characterized by a high temperature mineral assemblage of olivine, Ca plagioclase, clinopyroxene, and/or orthopyroxene that lacks hydrous phases, and which have granulitic textures, are assumed here to have been metamorphosed at granulite facies temperature conditions at shallow depths. The term "granulite facies" is applied to such rocks.

Breccias were defined as intervals of angular fragments in which clast rotation or relative displacement could be documented. Their characteristics were recorded in the ROCKY database. Portions of the core crosscut by dense vein networks may appear to be "brecciated," but if adjacent domains separated by the veins were not visibly rotated or displaced relative to one another they were described as net or mesh veined (see "Structural Geology," this chapter). Breccia samples were characterized on the basis of coherence, tectonic or sedimentary origin, and on the distribution of monogenic or polygenic clast distribution. Breccia descriptions included clast lithology, matrix mineralogy, secondary mineralogy, and abundance of clasts. Lithologic types, alteration mineralogy, and secondary phases were also recorded.

### Thin-section Description

Detailed petrographic descriptions were made aboard ship to aid identification and characterization of metamorphic mineral assemblages. Stable mineral parageneses were noted, as were textural features of minerals indicating overprinting events (e.g., coronas, overgrowths, and pseudomorphs). Mineral abundances were either visually estimated or determined by point counting. For each thin section, textures of metamorphic minerals were described. This information was recorded in the ROCKY database. The modal data allowed accurate characterization of the intensity of metamorphism and helped to establish the accuracy of the macroscopic and microscopic visual estimates of alteration extent.



## STRUCTURAL GEOLOGY

### Introduction

The cores recovered from Sites 920 and 921 in the MARK area on Leg 153 contribute to our understanding of the structure and tectonic evolution of oceanic lithosphere in a slow-spreading ridge environment. The priorities of the structural studies on Leg 153 included the following:

1. Document all igneous, metamorphic, and deformation structures in the core, by carefully describing their individual physical characteristics and their crosscutting relationships.
2. Record the orientation of all structures on the core face and orient them in three dimensions with respect to the core reference frame or in a geographic framework using data from paleomagnetic studies.
3. Use structural characteristics and other data to determine deformation processes, the conditions of deformation, and strain paths during oceanic lithosphere accretion and evolution.
4. Constrain the geometry and structural history of extension in the MARK area by using the above data, and evaluate the existing models and/or propose new models for crustal extension and exhumation of deep crustal and mantle rocks at the seafloor.

Although structural studies have been conducted on recent ODP expeditions (e.g., Legs 118, 131, 135, 140, 141, 147, and 148), there has been little standardization of methods and nomenclature. In addition, the nature of recovered lithologies and structures has varied significantly at different sites, requiring modifications to the existing structural methods and nomenclature. Classification schemes and nomenclature for rocks recovered in the MARK area were modified from those used previously.

### Overview of Macroscopic Core Description

Sketches of the core were drawn onto a Structural Visual Core Description (SVCD) template, used in conjunction with a spreadsheet. The SVCD provided two scaled columns for basic core-log sketches, annotations, and the locations of measurements (Fig. 8). Spreadsheet forms (Fig. 9) were used for hand-written recording of specific structures and measurements during core description. These data were subsequently entered into the corresponding electronic spreadsheet. The structures and measurements were cross-referenced to exact locations on the SVCD by abbreviated terms and numbers (Fig. 8). Descriptions were based on observations in both the working and the archive halves of the core, but measurements primarily were taken on the archive half. An additional summary spreadsheet provided a template for a piece-by-piece summary of deformation characteristics (Fig. 10). The summary spreadsheet was electronically linked to metamorphic and igneous spreadsheets that were based on similar piece-by-piece descriptions. The format of the detailed structural spreadsheet allowed multiple entries per piece, precluding direct electronic links to the piece-by-piece descriptions in the igneous and metamorphic spreadsheets. The primary and secondary structures for each core section and any additional comments were entered into the ROCKY database. Veins and vein sets for each core section were noted for their orientations relative to the primary and secondary structures and their crosscutting relations. Orientations of veins recorded during core description were mainly recorded as apparent dip data. True vein orientations relative to the core reference frame were not calculated until the end of core descriptions. These data are available on the structural spreadsheets (see CD-ROM section below) but were not entered in the ROCKY database. The layout of spreadsheet forms was modified slightly to suit the dominant structural features encountered at each site.

## Nomenclature

### Structural Identifiers

To maintain consistency of core descriptions we devised a set of structural feature "identifiers" to be entered into the spreadsheet (Fig. 11). Brittle deformation identifiers included fractures, joints, veins, faults, zones of brecciation, and any drilling-induced features. Definitions of these features were based on the sense of displacement across the discontinuities, evidence for shear displacement, and fracture-filling phases. The terminology adopted generally follows that of Twiss and Moores (1992). Joints (J) were defined as planar discontinuities with or without discernible opening. Veins (V) were defined as extensional or obliquely opening fractures with minor shear displacements, filled with any epigenic minerals. Faults (F) were defined as fractures with kinematic evidence for shear displacement across a discrete discontinuity. Breccia zones (B) were defined as zones of angular rock fragments separated by fracture networks with or without evidence for shear displacements. Core-scale dikes (D) were identified on the basis of the ability of the observer to infer the full width of the dike from intersections of chilled margins with a core piece or pieces. Igneous contacts (Ic) were recorded when a dike width could not be established. The term "magmatic vein" was adopted as an identifier for compositionally distinct mineral segregations that transect the peridotites and gabbros concordantly or discordantly. These segregations were distinguished from compositional banding (see below) by having constituents that are not common in the wall rocks. The boundaries of the magmatic veins range from sharply defined to very diffuse. Discontinuous trails of minerals were also included under this identifier. Where such compositionally distinct segregations contain metamorphic phases and igneous phases could no longer be identified, they were interpreted as hydrothermally altered magmatic veins.

Distinctions between drilling-induced features and natural structures were not always straightforward. Some structures were induced by drilling disturbances but others may have been generated by processes such as stress release, desiccation, and fluid expansion. Adopting recommended procedures from previous legs (Shipboard Scientific Party, 1991, 1992), if planar surfaces were mineralized, polished, or contained linear grooves, then a tectonic origin was inferred. The origins of unsealed breccias and gouges and isolated small pieces (typically pebble size or smaller) were problematic. If there was any doubt as to the origin of these various features, no structural measurements were made on them. In general, the recommendations of Lundberg and Moore (1986) were followed insofar as they were applicable to hard-rock features.

For the purposes of visual core description, mesoscopic ductile deformation was defined as more or less uniformly distributed flow without loss of cohesion (Rutter, 1986). No particular deformation mechanism is implied by this term. Foliations and lineations (Fig. 11) defined by magmatic flow fabrics (M) and crystal-plastic fabrics (Pf), foliations defined by anastomosing serpentine veins (Af), and cleavages, which included disjunctive cleavages (Dc) and crenulation cleavages (Cc), and folds (Fo), were identified in the cores. These designations generally follow the recommendations of Twiss and Moores (1992). Anastomosing foliation was assigned to foliations spaced at a millimeter scale, whereas disjunctive cleavage was assigned to foliations, anastomosing or planar, spaced on a centimeter scale. Magmatic fabrics were differentiated from crystal-plastic fabrics by the presence of aligned, unstrained minerals. Thin sections were used to confirm the strain-free character of grains. The term "mineral-shape fabric" (MF) was used to describe the preferred orientation of minerals (foliations or lineations) when a distinction could not be made between magmatic and crystal-plastic fabrics. Shear zones (Sz) were recorded where intense crystal-plastic fabrics localized within a core piece and kinematic evidence for shear displacements was present. An additional shear zone identifier (BS) was introduced for gabbroic lithologies at

	A	B	C	D	E	F	G	H	I	J	K	L	M	N	O	P
1	Hole	Core	Type	Section	Piece	Interval		Drillers Top of Core	ODP Lith Unit	Curatorial Piece Length	Depth to Top of Piece/Contact	Rock Name	Depth to Contact	Length Cored	Length Recovered	Recovery
2						Curatorial Top	Curatorial Bottom									
3						(cm)	(cm)	(mbsf)					(mbsf)	(m)	(m)	%
4	921C	1 R		1	1	0	10.5	2495	1	10.5	0	Gabbro	0	10	0.31	3.1
5	921C	1 R		1	2	12.5	28		1	15.5	0.125	Gabbro	0.125			
6	921C	1 R		1	3	29	34		1	5	0.29	Gabbro	0.29			
7	921C	2 R		1	1	0	11	2505	2	11	10	Diabase	10	9.6	1.305	13.59375
8	921C	2 R		1	2	12	15		2	3	10.12	Diabase	10.12			
9	921C	2 R		1	3	16	22.5		2	6.5	10.16	Diabase	10.16			
10	921C	2 R		1	4	23	32		2	9	10.23	Diabase	10.23			
11	921C	2 R		1	5	34	40		3	6	10.34	Deformed gabbro	10.34			
12	921C	2 R		1	6	41	52		3	11	10.41	Altered deformed gabbro	10.41			
13	921C	2 R		1	7	53	56.5		3	3.5	10.53	Deformed gabbro	10.53			
14	921C	2 R		1	8	57	69		3	12	10.57	Deformed gabbro	10.57			
15	921C	2 R		1	9	70	78		3	8	10.7	Deformed gabbro	10.7			
16	921C	2 R		1	10	78.5	88.5		3	10	10.785	Deformed gabbro	10.785			
17	921C	2 R		1	11	90	100		3	10	10.9	Deformed gabbro	10.9			
18	921C	2 R		1	12	101.5	103		3	1.5	11.015	Deformed gabbro	11.015			
19	921C	2 R		1	13	105	109		3	4	11.05	Deformed gabbro	11.05			
20	921C	2 R		1	14	110	124.5		3	14.5	11.1	Deformed gabbro	11.1			
21	921C	2 R		1	15	126	133.5		3	7.5	11.26	Deformed gabbro	11.26			
22	921C	2 R		1	16	134.5	138		3	3.5	11.345	Altered gabbro	11.345			
23	921C	2 R		2	1	0	9		3	9	11.5	Gabbro	11.4			
24	921C	2 R		2	2	10.5	12.5		3	2	11.605	Gabbro	11.505			
25	921C	2 R		2	3	14	17.5		3	3.5	11.64	Gabbro	11.54			
26	921C	2 R		2	4	18.5	22.5		3	4	11.685	Gabbro	11.585			
27	921C	2 R		2	5	23.5	31.5		4	8	11.735	Olivine gabbro	11.635			
28	921C	2 R		2	6	32.5	49		4	16.5	11.825	Olivine gabbro	11.725			
29	921C	2 R		2	7	51	81.5		4	30.5	12.01	olivine gabbro	11.91			
30	921C	2 R		2	8	83	94.5		4	11.5	12.33	Olivine gabbro	12.23			

Figure 7. Example of curatorial log (CURLOG) data recording template for Leg 153.

	Q	R	S	T	U	V	W	X	Y	Z	AA	AB	AC	AD	AE	AF	AG	AH	AI	AJ	AK	AL	AM	AN	AO	AP	AQ	AR	AS	AT	AU					
1	SHIPBOARD ANALYSIS					SAMPLING BY SHIPBOARD SCIENTISTS																														
2	XRF	TS	PM	PP	XRD																															
3	(cm)	(cm)	(cm)	(cm)	(cm)	AGAR	AGRI	CANN	JFC	CEU	DIL	FLE	NORI	GAG	GEE	JAN	HUR	KAR	DSK	PAM	LAW	VES	JAY	MUT	KIYO	PEZ	KENT	STE	WEIS	CARL	WHI					
4																																				
5																																				
6		29																																		
7	3	7																																		
8																																				
9																																				
10																																				
11																																				
12																																				
13																																				
14																																				
15																																				
16																																				
17																																				
18																																				
19																																				
20		113		113																																
21		127																																		
22																																				
23		6																																		
24																																				
25																																				
26																																				
27																																				
28																																				
29		61																																		
30																																				

Figure 7 (continued).



### Structure Visual Description

Leg 153    Hole 920D    Core 4    Section 3    Observer YRD

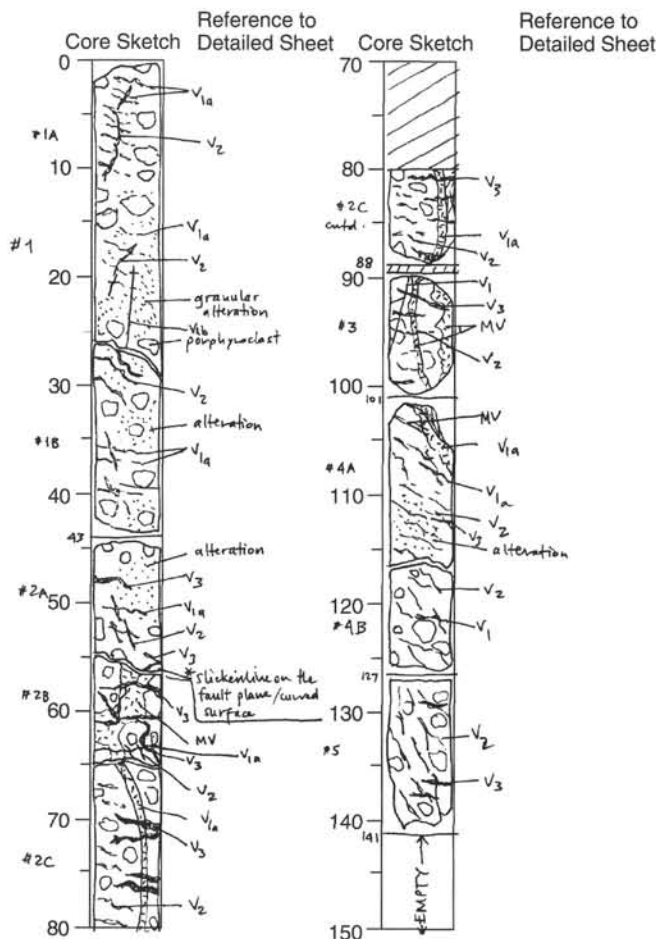


Figure 8. An example of the structural visual core description form (SVCD) used to record the location of geometry and structures to scale. Letters and subscript numbers refer to specific features in the core (see text for discussion). These data are contained on the CD-ROM (back pocket, this volume) in the "STRUCTUR" directory.

Sites 921, 922, 923, and 924, to designate a particular textural association consisting of angular fragments of igneous phases (commonly clinopyroxene) surrounded by a meshwork of veins commonly composed of plagioclase. The vein phases are commonly finer grained but mineralogically similar to the constituents of adjacent undeformed gabbro. The mesoscopic relations (also confirmed in thin sections) suggest grain-scale fracturing either synchronous with or overprinted by crystal-plastic deformation.

Compositional layering (CL) was also included in the structural spreadsheet. In some instances it was difficult to determine whether mineralogically distinct zones with gradational boundaries were defined by compositional layering or alteration. In these cases the orientations of the planar gradational boundaries (Gb) were recorded and accompanied by explanatory remarks. In the gabbroic units of Sites 921, 922, 923, and 924, textural and compositional variations could not always be distinguished from one another and may coincide. The term "compositional and/or textural variation" (CTV) was assigned to the location of gradational or discrete boundaries that did not qualify as repeated compositional layers and did not necessarily involve any change in composition across the boundary. These features are often irregular and could not be oriented as a planar boundary. Igneous contacts were recorded where clear intrusive relations are

preserved. Additional identifiers were used in the structure spreadsheets for undeformed gabbro pieces, fine-, medium-, and coarse-grained textures (FGE, MGE, and CGE). These identifiers were used solely to describe textures on a piece-by-piece basis for compatibility with the igneous and metamorphic spreadsheets. In general, these were used only in the absence of other identifiers. For each identifier a planar and/or linear orientation was recorded. Additional columns on the spreadsheet noted other details and comments. A checklist was used to ensure uniformity of explanatory remarks (Fig. 12).

### Fabric Intensities and Textural Terms

A key for fabric “intensity” and a list of textural abbreviations refined identifier descriptions (Fig. 13). When feasible, (semi-) quantitative estimates of feature development were used to define a five-category relative “intensity scale.” This scale is based on different characteristics for different types of structures and not all of the identifiers could be assigned an intensity value. The intensity estimates are only qualitative. Shipboard structural geologists used the following list to ensure consistency during core description:

1. For joints and faults, the intensity scale relates to frequency and spacing (i.e., density) estimated by the linear intercept method along the central divide of the core piece. If a piece was not oriented, spacing was estimated along the long axis of the piece. As no three-dimensional corrections were applied, these values remain semi-quantitative.
2. Vein intensity is related to an estimation of percentage of veining on the cut face of the archive half of the core. In contrast to other intensity scales, the vein scale has been subdivided into seven groups so that the relatively low percentages encountered during Leg 153 could be distinguished. The densities of vein arrays were also recorded separately on the spreadsheet.
3. Brecciation intensity relates to the relative percentage of clasts to matrix.
4. Foliation intensities, other than crystal-plastic foliation, broadly relate to the spacing of foliation planes. In the case of an anastomosing foliation, the closer the foliation planes and the more planar they become, the higher the intensity value.
5. Crystal-plastic fabric intensities related to the attenuation and degree of preferred alignment of porphyroclasts and the degree of preferred alignment of any mineral grains.
6. Fold intensity relates to the interlimb angle for individual or multiple folds.
7. Layering intensity relates only to the layer width and was applied to any repeated layers with discrete or gradational boundaries. Such layers include primary magmatic layering, alteration or grain-size variations.
8. Magmatic deformation intensity relates broadly to the degree of shape preferred orientation of magmatic phases.

### Textural Terms

Eight textural classes were selected for the purpose of mesoscopic description (Fig. 14). These classes do not necessarily directly relate to any single physical parameter, such as stress or strain. Moreover, some of these terms apply only to mafic rocks, others to ultramafic rocks, and some to both of them. The primary reason for selecting these classes was that they are relatively unambiguous textural terms (Mercier and Nicolas, 1975; Rutter, 1986; Twiss and Moores, 1992). The definitions were used primarily for hand-sample observations where thin sections were not necessarily available. Protogranular refers to the centimeter-sized clusters of interlocking olivine, pyroxenes, and spinels in peridotites, with little or no evidence for grain-scale deformation. Coarse-grained equigranular refers to a peridotite that has been deformed but shows no marked grain-size reduction. Porphyroclastic refers to a polymodal grain-size distribution; medium-grained (1–5 mm) more or less elongated porphyroclasts are embed-

LOG					FEATURE	POSITION		VEINS					PLANAR			LINEAR		CORR ORIENT	FAULTS					COMMENTS	
Hole	Core	Section	Piece	Orient?	Identifier	Texture Intensity	Top	Bottom	Center	Mineralogy	est. % area	Array Density (#/m)	Width (mm)	Length (mm)	Apparent dip = dr	Apparent dip = dr/2	Strike	Dip	Plunge & Trend	Strike & Dip	Plunge & Trend	Nature of Fault Rock	App. Shear Sense	Zone Thickness	Displacement (mm)
920B	BR	3	7	Y	F	1	62.5	66	64							180	40				sheared serpentinite	N	7	10	
920B	BR	3	10	Y	PF	2										180	40								Piece 9 same but unoriented
920B	BR	3	10	Y	AF	1										180	40								
920B	BR	3	10	Y	V1	1				serpentine	1	<1				180	40								
920B	BR	3	10	Y	V2	1				serpentine	<1	1				0	70								
920B	BR	3	11	Y	F	1	105	109	107							180	40				sheared serpentinite	N	3		
920B	BR	3	12	N	PF	PC	1																		
920B	13R	3	2	y	v2	1				White serp.	0.3	1	10	58/090	41/180	29	61								segmented and overlapping en-echelon segments
920B	13R	3	2	y	v3	1				light gm. serp.		0.5	20	90/0	0/183	3	90								cuts across v1
920B	13R	3	2	y	v4	1				White and gm. serp.		8	45	9/090	17/180	63	19								single vein is shated along and within it
920B	13R	3	2	y	v5	1				blue-white serp.		0.5	53	10/270	30/180	107	31								grain size boundary between coarse-grained and med. grained material
920B	13R	3	5	4	3	y	GB							57/270	37/000	206	60								cuts across the grain size boundary
920B	13R	3	5	4	3	y	v1	1		white drusy?		15	57	9/090	26/000	288	27								cuts across all the fabric and the piece is broken along the joint plane
920B	13R	3	5	4	3	y	J	1				1	125	63/090	59/180	40	69								light band across center of piece
920B	13R	4	2	Y	A/CL	3	10	16.2	12.5					8/090	48/000	277	48								L-S Tectonite, strong amph. lineation
920B	13R	4	2	Y	PI	MG	3							70/270	175	175	70								L-S Tectonite, Piece 3 similar to #8 & 9, very weak foliation
920B	13R	4	3	Y	PI	MG	3							12/090											seems to reflect grain size variations NB perpendicular to lineation
920B	13R	4	3	Y	D1	1				meta gabbro		3	90	70/270	206	206	72								subparallel to amph fabric, deformed-cut by v1!!
920B	13R	4	3	Y	v1	T	17	19	18	plag?		3	50	17/090											v1 cuts D1
920B	13R	4	4	Y	PI	3								74/270				82/195							L-S Tectonite
920B	13R	4	4	Y	v1	1								74/270	197	197	75								
920B	13R	4	4	Y	v2	1						2	85	75/270											metagabbro contact with microgneiss
920B	13R	4	5	Y	IC	3	41	48	46					50/270	154	154	53								L-S Tectonite
920B	13R	4	5	Y	PH	MG	3									65/216									

Figure 9. An example of the spreadsheet devised for the computer storage and manipulation of structural data derived from the core description. The full original measures 50 × 17 cm and occupies two U.S. letter-sized sheets. A more manageable version of the spreadsheet, containing the most frequently used columns for each hole, was used as a working spreadsheet. The complete set of final electronic spreadsheets is contained on the CD-ROM (back pocket, this volume) in the "STRUCTUR" directory.

	A	B	C	D	E	F	G	H	I	J	K	L	M	N	O	P	Q	R	S	T	
1	CURATORIAL DATA						ROCK DESCRIPTION			DEFORMATION INTENSITY										ADDITIONAL COMMENTS	
	Hole	Core	Section Number	Piece Number	Top of piece	Depth to top of piece	ODP lithological unit	Rock Name	Total Alteration	Joints	Veins	Breccias/Cataclases	Faults	Plastic fabrics	Magmatic fabrics	Partitioning of brittle defm.	Partitioning of duct. defm.	Predom. vein mineral.	Meta. texture		
2																					
3					(cm)	(mbsf)			%												
4	921C	1	1	1	0	0.0	1	Gabbro	33	0	1	1	0	0	0	1	0	2,6,12	0		
5	921C	1	1	2	13	0.1	1	Gabbro	28	0	0	3	0	0	0	1	0	2,6,12	0		
6	921C	1	1	3	29	0.3	1	Gabbro	33	0	0	3	0	0	0	1	0	2,6,12	0		
7	921C	2	1	1	0	10.0	2	Diabase	4	1	1	0	0	0	0	1	0	5	0		
8	921C	2	1	2	12	10.1	2	Diabase	0	0	0	0	0	0	0	0	0	0	0		
9	921C	2	1	3	16	10.2	2	Diabase	0	0	1	0	0	0	0	1	0	5	0		
10	921C	2	1	4	23	10.2	2	Diabase	0	0	1	0	0	0	0	1	0	5	0		
11	921C	2	1	5	34	10.3	3	Deformed gabbro	90	0	0	0	0	0	0	0	0	0	0		
12	921C	2	1	6	41	10.4	3	Altered deformed gabbro	90	0	1	0	0	0	0	1	0	5	0		
13	921C	2	1	7	53	10.5	3	Deformed gabbro	76	0	1	0	0	0	0	1	0	5	0		
14	921C	2	1	8	57	10.6	3	Deformed gabbro	0	0	0	0	0	0	1	1	0	3,5	0		
15	921C	2	1	9	70	10.7	3	Deformed gabbro	0	0	0	0	0	4	1	0	1	0	0		
16	921C	2	1	10	79	10.8	3	Deformed gabbro	0	0	1	0	0	0	0	1	0	5	0		
17	921C	2	1	11	90	10.9	3	Deformed gabbro	0	0	0	0	0	0	0	0	0	3,5	0		
18	921C	2	1	12	102	11.0	3	Deformed gabbro	0	0	0	0	0	0	0	0	0	0	0		
19	921C	2	1	13	105	11.1	3	Deformed gabbro	0	0	1	0	0	0	0	1	0	5	0		
20	921C	2	1	14	110	11.1	3	Deformed gabbro	48	0	0	0	0	0	1	0	0	0	0		
21	921C	2	1	15	126	11.3	3	Deformed gabbro	15	0	1	0	0	0	1	1	0	3,5	0		
22	921C	2	1	16	135	11.3	3	Altered gabbro	0	0	0	0	0	0	0	0	0	0	0		
23	921C	2	2	1	0	11.5	3	Gabbro	27	0	1	0	0	0	0	1	0	12	0		
24	921C	2	2	2	11	11.6	3	Gabbro	18	0	0	0	0	0	0	0	0	0	0		
25	921C	2	2	3	14	11.6	3	Gabbro	28	0	1	0	0	0	0	1	0	12	0		
26	921C	2	2	4	19	11.7	3	Gabbro	22	0	1	0	0	0	0	1	0	12	0		
27	921C	2	2	5	24	11.7	4	Olivine gabbro	13	1	0	0	0	0	0	0	0	0	0		
28	921C	2	2	6	33	11.8	4	Olivine gabbro	3	0	0	0	0	0	0	0	0	0	0		
29	921C	2	2	7	51	12.0	4	Olivine gabbro	4	0	1	0	0	0	0	1	0	12	0		
30	921C	2	2	8	83	12.3	4	Olivine gabbro	4	0	1	0	0	0	0	1	0	12	0		

Figure 10. Example of structural summary (STRUCSUM) data recording template for Leg 153.

Structural identifiers, Leg 153			
Identifier	Abbrev.	Planar features	Linear features
Drilling Induced	DI		
Joints	J	Joint surface	
Veins	V	Vein margin, tip-lines of arrays	
Magmatic Vein	MV	Vein margin	
Dikes	D	Dike margin	
Faults	F	Fault plane	Slickenlines
Breccias	B	Zone margin/foliation	Slickenlines
Anastomosing Foliation	Al	Foliation plane	Slickenlines
Disjunctive cleavage	Dc	Cleavage plane	
Crenulation cleavage	Cc	Cleavage plane	
Folds	Fo	Fold hinge plane	Fold hinge line
Brittle Shear Zone	Bs	Shear zone margin	
Shear Zone	Sz	Shear zone margin	Mineral and intersection lineations
Crystal-Plastic Fabric	Pf	Shear zone margin/ foliation plane	Mineral and intersection lineations
Magmatic Fabrics	M	Foliation plane	Mineral and intersection lineations
Mineral Shape Fabric	MF	Foliation plane	Mineral and intersection lineations
Compositional and /or Textural Variation	CTV	Surface between zones of contrasting texture and/or composition	
Gradational Boundary (alteration/composition/ grainsize)	Gb	Approximate planar boundary orientation	
Compositional Layering	CL	Interlayer surfaces	
Igneous Contacts	Ic	Contact surface	
Undeformed gabbros	FGE	No measurement	
Undeformed gabbros	MGE	No measurement	
Undeformed gabbros	CGE	No measurement	

Figure 11. Key to structural identifiers used in structural VCD and spreadsheets on Leg 153. See text for discussion.

ded in a finer grained matrix. Gneissic refers to compositional banding in a ductilely deformed rock, where porphyroclasts are commonly elongated parallel to the banding. Schistose refers to the visibility of platy or prismatic metamorphic minerals that define a shape preferred orientation and typically a parallel fissility. The terms mylonitic, ultramylonitic, and cataclastic were used in accordance with the definitions presented by Twiss and Moores (1992).

### Structural Measurements

Structural features were recorded relative to position in the core section, including the piece(s) that contained them. The position was defined as the point where the structure intersects the central divide of the cut face of archive half of the core (Fig. 15A). Depths were measured from the top of the core section in centimeters. If the structure extends over an interval, then the depth of the top and the bottom of the feature were recorded. A representative orientation was taken to measure all the component structures (e.g., for vein arrays) for composite structures, as time allowed.

Apparent fault displacements were recorded as they appear on the cut face of the archive half of the core and the ends of broken pieces. Displacements seen on the core face were treated as components of dip-slip displacements, either normal or reverse. Displacements of features visible on the upper and lower surfaces of core pieces were treated as components of strike-slip and termed sinistral or dextral.

Displacements were generally measured between planar markers that had been displaced, parallel to the trace of the fault. If additional cuts and slickenside orientations were available, then these were used to differentiate between apparent dip-, oblique-, and strike-slip.

Structures were oriented with respect to the core reference frame. The convention we used for the core reference frame was as follows: The direction at 90° to the cut face of the archive core toward the curved surface was designated as 180°. The direction at 90° to the cut face of the working core toward the curved surface was therefore 000°. With the archive core oriented for way-up, the right side of the core was designated as 270° and the left side of the core was designated as 090° (Fig. 15). All spreadsheet orientations are given in the core reference frame unless otherwise noted.

Planar structures were oriented using the techniques outlined in Leg 131 (Shipboard Scientific Party, 1991). We employed the simple device suggested by Neil Lundberg that facilitates rapid, accurate measurements. This device consists of a simple protractor with a graduated scale and pivoted measuring arm (Fig. 12, "Explanatory Notes," Shipboard Scientific Party, 1991). Apparent dip angles of planar features were measured on the cut face of the archive half of the core. To do this, the base of the protractor was aligned parallel to the core axis and the measuring arm rotated into alignment with the feature of interest. The numbering on the graduated scale is opposite to that on most protractors, in that when the pivoted arm is horizontal it reads 00° and when it is vertical it reads 90°; this allows the dip to be read directly.

In order to obtain a true dip value, a second apparent dip reading was obtained where possible in a section perpendicular to the core face (auxiliary plane), aligning the protractor arm with the trace of the dipping feature in the outer wall of the core piece (Fig. 12, "Explanatory Notes," Shipboard Scientific Party, 1991). Apparent dips in the cut plane of the archive core were recorded as a two digit number (between 00° and 90°) with a dip direction to 090° or 270°. In the "auxiliary" plane (usually 90° to the cut face of the archive core) apparent dip directions were recorded as either 000° or 180°. The dip and the dip direction for the archive half of the core were recorded on the spreadsheet together with the auxiliary plane measurements.

Where structures were not evident in the auxiliary plane, the corresponding part of the structure was located in the working half of the core. A saw cut made at right angles to the main core face, or existing fracture surfaces in the core were used to make the second apparent dip measurement. In this case, the orientation of the saw cut or the fracture surface was recorded as the auxiliary plane azimuth and the auxiliary plane dip. The orientation of the structure was recorded as the apparent dip and dip direction in the auxiliary plane. If the working azimuth (strike in the core reference frame) of a structure was evident, for example at the end of a core section, then this azimuth was combined with the apparent dip measurement to calculate the true dip of the structure. If the structure was exposed in three dimensions and the true dip and working azimuth could be measured, then these were entered directly into the spreadsheet.

The two apparent dips and dip directions measured for each planar feature were used to calculate a plane. These calculations were performed by a Pascal program, LinesToPlane, written for a Macintosh personal computer by S.D. Hurst (CD-ROM, back pocket, this volume). This program can write files that can be read directly into the stereonet plotting program of R.W. Allmendinger (1988–1992), StereoNet version 4.6.

Where broken surfaces exposed lineations or striations, the plunge and trend was measured directly, relative to the core reference frame. Although no fold hinges were found in the cores, we recommend the technique by which hinge lines are identified in two mutually perpendicular sections. A pin used to connect the same inflection point exposed on the two surfaces (Fig. 16, "Explanatory Notes," Shipboard Scientific Party, 1992). The orientation of the pin was recorded as a pitch in a plane containing both the pin and a north-south horizontal line (in core reference frame). The dip of the plane measured



## COMMENTS CHECKLIST

The following is a checklist of structural characteristics that were searched for in macroscopic core samples. These characteristics supplement the information required by the spreadsheet and were noted in the comments section of the spreadsheet.

The feature-identifier code and a number corresponding to the  $n$ th feature in the each piece of the core is entered in the Identifier column of the spreadsheet and in the comments if needed (i.e.V3). The feature identifier is cross-referenced to the sketch in the visual core description.

### Joints

- joint density;
- plume structures on joint surface.

### Faults

- fault-zone thickness;
- nature of gouge (e.g., spatial variations in grain size), shear-sense from Riedel shears or fiber bundles on fault plane (stepping direction of secondary minerals).

### Veins

- orientation of individual veins and vein-array boundaries;
- magnitude and nature of offset;
- density of vein network;
- array characteristics:
  - ~ shear-sense
  - ~ angle between new vein segments and array boundary (measure of array dilatation);
- vein-filling minerals;
- internal structure of fibers;
- crack-seal structures and number of vein-opening events;
- wall-rock alteration and shape;
- vein terminations (splayed or tapered).

### Cataclastic Fabrics

- grain-size characteristics:
  - ~ grain shapes,

- ~ internal structure of clasts,
  - ~ composition of clast(s);
- spacing and number of fracture sets (if present);
- matrix material (gouge or secondary minerals).

### Crystal-Plastic Fabrics

- L-, LS- and S-tectonite;
- shear-sense indicators: block-rotated porphyroclasts, obliquity between lattice (cleavages in porphyroclasts) and shape fabrics, asymmetric augen, SC cleavage, discrete shear bands, mica fish, piggy-back porphyroclasts, and tension-gash arrays;
- Deformation mechanisms in each of the main rock-forming minerals: cataclasis or microfracturing, pressure solution and general crystal-plastic strain;
- mineralogical segregation or banding;
- grain-size characteristics:
  - ~ neoblast, porphyroclast,
  - ~ neoblast/porphyroclast ratio(s);
- nature and scale of strain partitioning through rock.

### Magmatic Fabrics

- shape or crystallographic preferred orientations as suggested by alignment of inequant minerals and twins;
- minerals that define the shape or lattice fabric;
- angle between shape fabric and layering plane

### Cleavages

- style of cleavage (e.g., crenulation, disjunctive);
- spacing or wavelength;
- angle between cleavage and earlier fabrics, noting directions of larger-scale fold closures.

### Folds

- exact inner-limb angle;
- estimate of hinge curvature (e.g., kink vs. round);
- asymmetry orientation of hingeline relative to other fabrics (e.g., stretching lineations, etc.);
- other geometrical aspects preserved in core (e.g.,

- wavelength, amplitude, etc.);
- profile sketch for VCD sheet;
- number of folds, if more than one.

### Compositional Layering/ Gradational Boundaries

- type of layering (e.g., sedimentary, igneous cumulate, alteration etc.);
- spacing between laminae.

### Igneous Contacts

- chilled margins (thickness, grain size, color);
- dike thickness.

### Cross-Cutting Relationships

- shear or orthogonal offset across fractures and veins;
- cross-cutting ductile fabrics vs. transposing ductile fabrics (angle between compositional layering and the ductile fabric);
- inclusion trails and fabrics in microlithon domains;
- intrusive relationships;
- sedimentary unconformities.

Figure 12. Table showing checklist used for spreadsheet comments associated with each structural identifier.


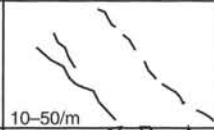
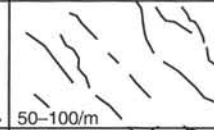
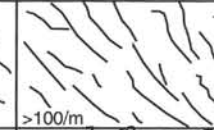

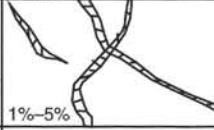
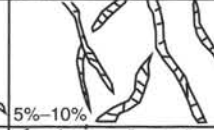
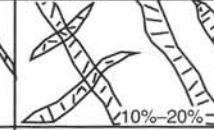
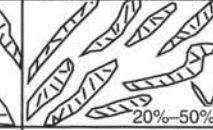
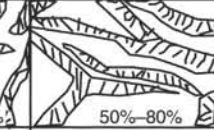
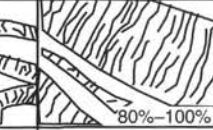
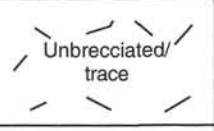


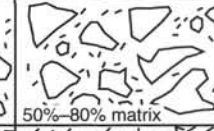

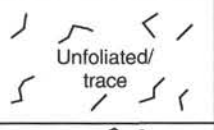

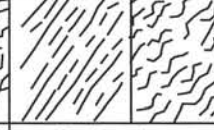
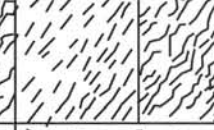





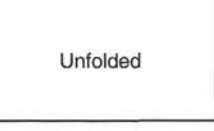
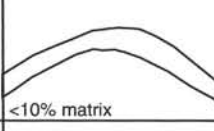

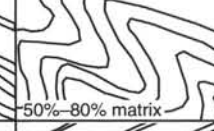

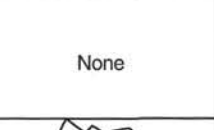
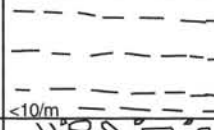

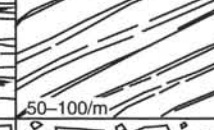
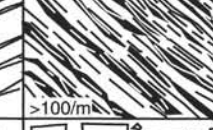





Features	0	1	2	3	4	5	6
		↔ 10 cm ↔					
Joints/faults							
		<10/m	10–50/m	50–100/m	>100/m		
Veins (% for each generation of veins)							
	Trace <1%	1%–5%	5%–10%	10%–20%	20%–50%	50%–80%	80%–100%
Breccias							
	Unbrecciated/ trace	<10% matrix	10%–50% matrix	50%–80% matrix	>80% matrix		
Foliations							
	Disjunctive (cm)	Anastomosing (mm)					
Crystal-plastic fabrics							
	None						
Folds							
	Unfolded	<10% matrix	10%–50% matrix	50%–80% matrix	>80% matrix		
Layering							
	None	<10/m	10–50/m	50–100/m	>100/m		
Magmatic fabrics							

Figure 13. Table showing intensity scales applied to structural identifiers for brittle deformation. See text for detailed explanation.

Textures	Code	Abbreviation
Protogranular	1	Pg
CG equigranular	2	Cge
Porphyroclastic	3	Pc
Elongate porphyroclastic	4	Epc
Mylonitic	5	My
Ultramylonitic	6	Um
Cataclastic	7	Ca
Equigranular gneiss	8	EG
Augen gneiss	9	AG
Schistose	10	Sh

Figure 14. Key to textural features entered in structural VCDs (abbreviation) and summary spreadsheet (number code).

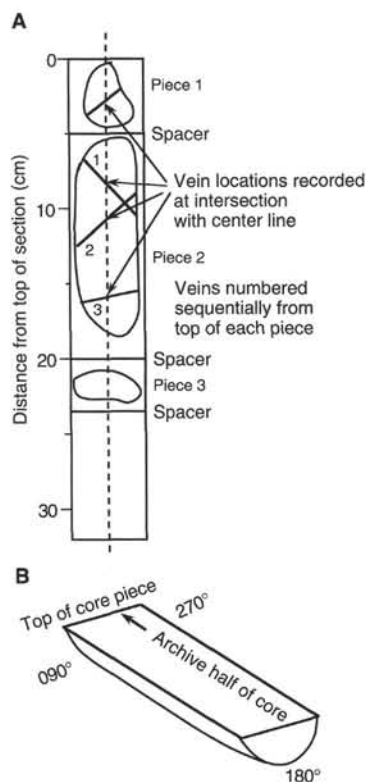


Figure 15. Core reference frame orienting structures showing convention for (A) numbering and (B) locating features.

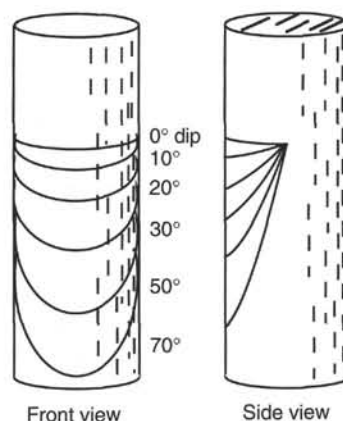


Figure 16. The structure measurement sleeve consists of a clear plastic tube that slides over the core and core liner; designed by S.D. Hurst. A series of semi-ellipses is marked at 10° increments on the tube that can be rotated and translated until they line up with the planar structure in the core. The dip of the plane is approximated and the strike relative to core coordinates is read off the azimuth markings around the 0° dip circle marked on the tube.

on the cut surface is therefore the true dip, and the strike is either 000° or 180°. Using the Allmendinger stereoplotting software, the strike closest to the pitch is entered, together with a dip and a dip direction for the plane and a value for the pitch.

Where long (>20 cm) core pieces were recovered, it was possible to employ a new device to measure true dips and strikes directly and rapidly. The device consisted of a clear plastic tube that slides over either the core or core liner (Fig. 16). A series of semi-ellipses are marked at 10° increments on the tube that can be rotated and translated until they line up with the planar structure in the core. The dip of the plane is approximated and the strike relative to core coordinates is read off the azimuth markings around the 0° dip circle marked on the tube.

### Thin-section Descriptions

Thin sections were examined to characterize the microstructural aspects of important mesoscopic structures in the core. Information that was obtained included microstructures of each mineral phase present, kinematic indicators, crystallographic and shape preferred orientations, and pre-, syn-, and postkinematic alteration features. The relative timing of microstructures was determined from overprinting or crosscutting relationships.

Thin sections were oriented, where possible, with respect to the core axis (original attitude of the vertical preserved). Selected samples were cut, perpendicular to the foliation and parallel to any stretching lineation in order to examine shear-sense indicators and the shape preferred orientation of minerals (Fig. 19, "Explanatory Notes," Shipboard Scientific Party, 1993). Thin-section descriptions of microstructures by the structural geologists were entered as comments in the ROCKY database.

The terms used to describe microstructures generally follow the recommendations of Twiss and Moores (1992); the terminology of Mercier and Nicolas (1975) was used for ultramafic rocks. Microstructures of the ultramafic rocks recovered at Site 920 are discussed in detail in the "Igneous Petrology" and "Structural Geology" sections of the "Site 920" chapter (this volume). The microstructures observed in the gabbroic rocks recovered at Sites 921, 922, 923, and 924 comprise a wide range of textural types that are not described in detail elsewhere. Although a broad and more or less continuous spectrum of microstructures occurs in the gabbroic rocks, for the purposes of entering data into spreadsheets a number of textural types characterized by specific microstructural styles were defined. These are described briefly below and summarized in Figure 17.



Textural group	Plagioclase	Olivine	Pyroxene
1 a b	>90% subhedral laths (2 to >10 mm); no deformation microstructures, magmatic twins only; random crystallographic orientation; well-defined shape preferred orientation	No deformation microstructures except local development of undulose extinction	No deformation microstructures
2 a b	70%–90% subhedral laths (2 to >10 mm); 10%–30% fine-grained (0.5 to 1 mm) mosaic; deformation twins present but uncommon; random crystallographic preferred orientation; well-defined crystallographic preferred orientation	Common sub-grain boundaries and undulose extinction	No deformation microstructures
3	>90% fine-grained mosaic (0.1–2 mm); deformation twins and undulose extinction common; moderate shape preferred orientation; strong crystallographic preferred orientation	Elongated aggregates of neoblasts (0.1–0.3 mm)	Bent and kinked grains absent to moderate; common to extensive neoblasts
4 a b	Strongly bimodal grain-size distribution; localized fine-grained neoblasts (<0.03–0.2 mm); polygonal neoblasts; sutured neoblasts	Closely-spaced subgrain boundaries; pervasive undulose extinction; extensive neoblasts	Bent and kinked porphyroclasts; localized neoblasts
5	common intracrystalline microfractures associated with very fine-grained neoblasts (average 0.05 mm); extensive bent, kinked and deformation twinned grains; pervasive undulose extinction		
6	intracrystalline and intercrystalline microfractures and gouge bands; extensive bent, kinked and deformation twinned grains, pervasive undulose extinction		

Figure 17. Table summarizing microstructural elements in the gabbroic rocks of Sites 921–924, based on thin-section descriptions. The textural groups indicate typical microstructural associations in a continuous spectrum of textures. No sharp boundaries between the groups are implied.

For gabbroic rocks, six textural groups were defined based on plagioclase and, to a lesser extent, olivine and pyroxene microstructures (Fig. 17). Textural Group 1 refers to magmatic rocks virtually devoid of evidence for crystal-plastic or brittle deformation; the other groups refer to rocks whose magmatic texture is overprinted by crystal-plastic and/or brittle deformation. These textures are detailed below and summarized in Figure 17.

**Textural Group 1:** More than 90% of the plagioclase occurs as subhedral elongated grains ranging from 2 to >10 mm. Twins are dominantly straight and regular (hereafter referred to as “magmatic twins”). Olivine and pyroxene occur as medium-grained interstitial crystals or as coarse oikocrysts. They do not show any intracrystalline deformation textures. Subgroup 1a refers to a random crystal orientation. Subgroup 1b refers to a well-defined shape fabric defined by alignment of plagioclase laths.

**Textural Group 2:** Plagioclase occurs both as euhedral laths and as patches of finer grained (0.5–2 mm) mosaic aggregates (i.e., anhedral equant grains showing 120° triple junctions). These mosaic aggregates commonly have the overall shape of plagioclase laths. Magmatic and deformation twins coexist. Sub-grain boundaries and undulose extinction are common in olivine crystals. Orthopyroxene and clinopyroxene grains are generally devoid of intracrystalline deformation features. Subgroup 2 refers to a random shape orientation and 2b to a well-defined shape preferred orientation.

**Textural Group 3:** Plagioclase occurs mainly (>90%) as a fine-grained (0.1–2 mm, average 0.5 mm) mosaic of anhedral grains. Grain boundaries are straight to slightly irregular and 120° triple junctions are common. Most of the twins are deformation twins. Grains are equant to slightly elongated. Shape preferred orientation is moderate, but the lattice fabric is generally strong. Olivine occurs as 0.1–0.3 mm neoblasts, scattered or forming elongated clusters likely derived from former porphyroclasts. Grains of both pyroxenes show moderate to strong grain-size reduction.

**Textural Group 4:** This textural group is characterized by non-penetrative grain-size reduction of minerals leading to the development of a strongly bimodal grain-size distribution. Grain-size reduction occurs along a network of high-strain zones that outline porphyroclasts. Plagioclase laths show deformation twins, undulose extinction, and may be bent. Plagioclase neoblasts are polygonal and show generally an extremely strong crystallographic preferred orientation. Plagioclase crystals range from <0.03 to 0.2 mm. The extent of plagioclase recrystallization varies widely within a single thin section. Olivine has closely spaced subgrain boundaries and pervasive undulose extinction. Pyroxene crystals are bent or kinked. There is moderate pyroxene grain-size reduction, generally restricted to the grain margins. Subgroups 4a and 4b have polygonal and sutured plagioclase neoblasts, respectively.

**Textural Group 5:** All the mineral phases are bent or kinked and contain intracrystalline microfractures. Very fine-grained (<0.03–0.1 mm) neoblasts develop locally adjacent to the fractures.

**Textural Group 6:** Rocks of this group are characterized by the extensive development of intracrystalline and intercrystalline microfractures and gouge bands. The intensity of microfractures and gouge bands is very heterogeneously developed.

### Data on CD-ROM

The CD-ROM (back pocket, this volume) contains the complete set of spreadsheets with piece-by-piece data for all structural features identified and measured. A set of summary spreadsheets that are linked to the igneous and metamorphic spreadsheets are also contained on the CD-ROM. Keys, summary tables, checklists, and thin-section summaries and notes are also archived. Compressed versions of the figures created for this volume, compatible with Macintosh computers, are located in the directories labeled REPT92X in the “Structure” directory. Scanned TIFF images of all the SVCD drawings are archived in the “STRCDRAW” file. Apparent dip data and

true strike and dip data for all measurable features are contained in the "STR\_DIP" subdirectory. This directory also contains the LinesToPlane documentation and program that converts the apparent dip data to true strike and dip in an archived form.

## PALEOMAGNETISM

Paleomagnetic measurements were performed on discrete minicore samples and on some continuous pieces of the archive half-core. A standard 2.5-cm-diameter minicore sample was generally taken from each section of core for shipboard study. Minicore samples were chosen to be representative of the lithology and alteration mineralogy, and an effort was made to select samples near important structural features for possible reorientation using the remanent magnetization directions. The azimuths of core samples recovered by rotary drilling are not constrained. All magnetic data are therefore reported relative to the following core coordinates: +X (north) points into the face of the working half of the core, +Y (east) points toward the right side of the face of the working half of the core, and +Z is down (Fig. 18).

The remanent magnetization of continuous core pieces was measured with the 2-G Enterprises (Model 760R) pass-through cryogenic rock magnetometer, operated in flux-counting mode. The superconducting quantum interference device (SQUID) sensors in the cryogenic magnetometer have a response function that is ~20 cm long. Declination and inclination data are derived from the effective measurement volumes for the three orthogonal sensors. An alternating field (AF) demagnetizer (Model 2G600) capable of producing an alternating field up to 25 mT was used on-line with the pass-through cryogenic magnetometer. The natural remanent magnetization (NRM) and the remanence after demagnetization (typically at 10 and 20 mT) were measured for all archive core sections.

Discrete samples were measured with the Molspin magnetometer, using the MolMac program (version 1.38.3). Most discrete samples were stepwise demagnetized using the Schonstedt AF demagnetizer (Model GSD-1). The sample was either demagnetized along the positive axis directions (+X, +Y, +Z) or the reverse axial directions (-X, -Y, -Z) at alternate demagnetization steps to facilitate recognition of any spurious anhysteretic remanence. A small number of samples were also thermally demagnetized by the Schonstedt Thermal Specimen Demagnetizer (Model TSD-1). Initial susceptibility was monitored between each temperature step as a means of assessing any irreversible mineralogical changes associated with heating.

Whole-core magnetic susceptibility ( $k$ ) was measured at 3-cm intervals on all sections using the Bartington Instrument susceptibility meter (Model MS1; 80 mm loop, 4.7 kHz, SI units) mounted on the multisensor track. Susceptibility measurements were made on the whole core following the establishment of the final curated positions and placement of spacers and are therefore directly comparable with the pass-through measurements of the archive half cores. The volume susceptibility of minicores was measured using the Kappabridge KLY-2. Susceptibility values on the Kappabridge are reported relative to a nominal volume of 10 cm<sup>3</sup>; all discrete sample susceptibilities reported here have been corrected for the calculated cylindrical sample volume. The volume susceptibility was used in conjunction with the NRM intensity to calculate the Koenigsberger ratio ( $Q$ , the ratio of remanent to induced magnetization) of the samples. The IGRF field value at the site (~38,500 nT = 30.63 A/m) was used for calculating  $Q$  ( $Q = \text{NRM [A/m]} / [k(\text{SI}) \times H(\text{A/m})]$ ), where  $H$  is the magnetic field).

The anisotropy of magnetic susceptibility (AMS) was determined for most shipboard samples, using the Kappabridge and the program ANI20 supplied by Geofyzika Brno. A 15 position measurement scheme is used to derive the susceptibility tensor ( $k_{ij}$ ) and associated eigenvectors and eigenvalues. In addition to standard paleomagnetic measurements, a small number of samples were given an anhysteretic remanent magnetization (ARM) and/or a stepwise isothermal remanence acquisition. The ARM was generated in an alternating field of 100 mT with

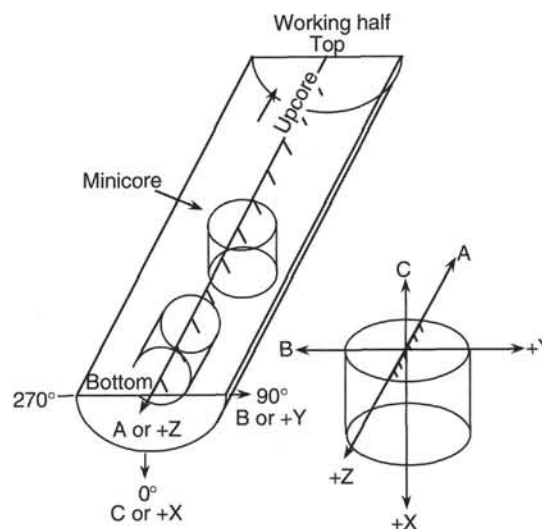


Figure 18. ODP orientation convention for paleomagnetic samples.

a bias field of 0.1 mT. Isothermal remanence (to a peak field of ~1.0 T) was imparted using an ASC Scientific impulse magnetizer.

The accompanying CD-ROM (back pocket, this volume) contains the complete set of paleomagnetic data measured aboard the *JOIDES Resolution* and includes whole core remanence, susceptibility, discrete sample measurements, and AMS. Data tables in ASCII form and compressed versions of figures used in all site chapters are stored in the "PMAGDATA" directory on the CD-ROM.

## PHYSICAL PROPERTIES

Physical property determinations from Leg 153 rocks are intended to provide further information on the lithologic and structural units identified at each hole and to provide a link between direct geological observations in slow-spreading environments and those inferred from a variety of geophysical methods.

Measurements of physical properties were made from the whole core as well as from standard 2.5-cm-diameter minicore samples obtained after the core was split. Whole-core section measurements of bulk density and magnetic susceptibility were made using MST. The MST consists of a GRAPE, a compressional-wave core logger (PWL), and a magnetic susceptibility monitor. Minicore samples, selected as representative of the core, were analyzed by the paleomagnetic group before determinations of compressional-wave velocity, thermal conductivity, electrical resistivity, and index properties (bulk density, grain density, water content, porosity, and dry density) were completed. Sampling frequency was generally one per core section. Selected minicores were powdered for subsequent analysis by XRF (see "Igneous Petrology," this chapter).

Further details on the techniques and methodologies used in the Leg 153 physical properties measurements program can be found in the Leg 147 "Explanatory Notes" and references therein (Shipboard Scientific Party, 1993). Physical properties data for Leg 153 holes are included in this volume's CD-ROM (back pocket).

## LINKED SPREADSHEETS AND DATABASE

The shipboard scientists devised a series of linked spreadsheets to facilitate data collection and manipulation (Fig. 19), which were constructed around a central curatorial spreadsheet (CURLOG) that contained all the sample curation information. Two spreadsheet forms were used to record the macroscopic description of "hard" rocks. Each of these spreadsheets is linked to the CURLOG (Fig. 7), which records curatorial information according to standard ODP format as

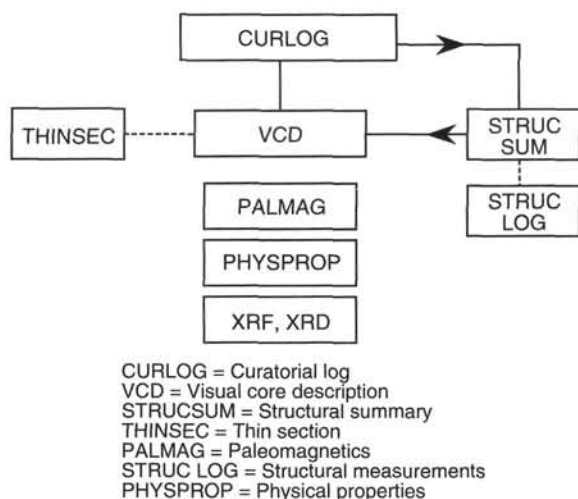


Figure 19. Flow chart for Leg 153 linked spreadsheets.

the initial step prior to core description. The curatorial data is then automatically displayed via embedded links in the macroscopic description spreadsheets. A summary spreadsheet for igneous, metamorphic, and structural macroscopic descriptions, called the VCD log (Fig. 20), was used to record observations of igneous features during initial core description. The VCD also summarized information via embedded links to a spreadsheet containing structural summary data (STRUCSUM; Fig. 10). The VCD log contains all the macroscopic descriptive data collected by the igneous petrologists. In addition, generic detailed thin-section spreadsheets (TSPERID for peridotite samples, TSGAB for gabbro samples) were created for igneous, metamorphic, and structural microscope observations. Codes in each spreadsheet, as discussed in the "Explanatory Notes" (this volume) are listed in the terminology spreadsheet (TERMINOL; Table 2). A stand-alone structural spreadsheet (STRUCLOG; Fig. 21) was created to store information on all structural measurements made during the leg. Paleomagnetic, physical properties, XRF, and XRD data were stored in separate tables.

The curatorial information includes leg, site, hole, core, type, section, piece, curatorial top and bottom of the piece (in centimeters), piece length (in centimeters), depth to the top of the piece (mbsf), depth to unit contact (mbsf), drillers depth to the top of each core, recovery data, rock unit number, and lithology of the piece from the VCD log. The completed spreadsheets are contained on the CD-ROM that accompanies this volume (back pocket).

Observations were recorded aboard ship onto spreadsheets by the igneous, metamorphic, and structural geologists and were used to complete the summary information entered into standard ODP hard-rock barrel sheets. The text for the barrel sheets was entered into the

ODP hard-rock description program ROCKY, which replaced the HARVI and HRTHIN archival programs used on previous legs.

## REFERENCES\*

- Best, M.G., 1982. *Igneous and Metamorphic Petrology*: New York (Freeman and Company).
- Dick, H.J.B., Erzinger, J., Stokking, L.B., et al., 1992. *Proc. ODP, Init. Repts.*, 140: College Station, TX (Ocean Drilling Program).
- Irvine, T.N., 1981. Terminology for layered intrusions. *J. Petrol.*, 23:127-162.
- Lundberg, N., and Moore, J.C., 1986. Macroscopic structural features in Deep Sea Drilling Project cores from forearc regions. In Moore, J.C. (Ed.), *Structural Fabric in Deep Sea Drilling Project Cores From Forearcs*. Mem.—Geol. Soc. Am., 166:13-44.
- McKenzie, W.S., Donaldson, C.H., and Guilford, C., 1982. *Atlas of Igneous Rocks and Their Textures*: New York (Longman Scientific & Technical; Wiley).
- Mercier, J.-C.C., and Nicolas, A., 1975. Textures and fabrics of upper-mantle peridotites as illustrated by xenoliths from basalts. *J. Petrol.*, 16:454-487.
- Rutter, E.H., 1986. On the nomenclature of mode of failure transitions in rocks. *Tectonophysics*, 122:381-387.
- Shipboard Scientific Party, 1989. Explanatory notes. In Robinson, P.T., Von Herzen, R., et al., *Proc. ODP, Init. Repts.*, 118: College Station, TX (Ocean Drilling Program), 3-23.
- , 1991. Explanatory notes. In Taira, A., Hill, I., Firth, J.V., et al., *Proc. ODP, Init. Repts.*, 131: College Station, TX (Ocean Drilling Program), 25-60.
- , 1992. Explanatory notes. In Behrmann, J.H., Lewis, S.D., Musgrave, R.J., et al., *Proc. ODP, Init. Repts.*, 141: College Station, TX (Ocean Drilling Program), 37-71.
- , 1992. Explanatory notes. In Dick, H.J.B., Erzinger, J., Stokking, L.B., et al., *Proc. ODP, Init. Repts.*, 140: College Station, TX (Ocean Drilling Program), 5-33.
- , 1993. Explanatory notes. In Gillis, K., Mével, C., Allan, J., et al., *Proc. ODP, Init. Repts.*, 147: College Station, TX (Ocean Drilling Program), 15-42.
- , 1993. Explanatory notes. In Rea, D.K., Basov, I.A., Janecek, T.R., Palmer-Julson, A., et al., *Proc. ODP, Init. Repts.*, 145: College Station, TX (Ocean Drilling Program), 9-33.
- Streckeisen, A., 1974. Classification and nomenclature of plutonic rocks. *Geol. Rundsch.*, 63:773-786.
- Twiss, R.J., and Moores, E.M., 1992. *Structural Geology*: New York (W.H. Freeman).
- Wager, L.R., Brown, G.M., and Wadsworth, W.J., 1960. Types of igneous cumulates. *J. Petrol.*, 1:73-85.
- Yardley, B.W.D., 1989. *An Introduction to Metamorphic Petrology*: New York (Longman, Harlow).

\*Abbreviations for names of organizations and publications in ODP reference lists follow the style given in *Chemical Abstracts Service Source Index* (published by American Chemical Society).



	A	B	C	D	E	F	G	H	I	J	K	L	M	N	O	P	Q	R	S	T	U	V	W	X	Y	Z	AA	AB
1	CURATORIAL DATA							ROCK DESCRIPTION							STRUCTURE										MINERALOGY			
	Hole	Core	Section Number	Piece Number	Top of piece	Piece Length	Depth to top of piece	ODP lith. unit	Rock Name Code		Percent Total Alt.	Metamorphic Facies	Equigranular Texture	Inequigranular Texture	Cumulate texture													
2																Color	Igneous layering	Metamorphic texture	Distrib.of Brittle Def	Brittle Intensity	Distrib. of Ductile Def	Ductile Intensity	Unit Contact Type	Vein Assemblage	Magmatic Veins	Olivine (%)	Crystal size	
3					(cm)	(cm)	(mbsf)																				max.	min.
4	921C	1	1	1	0	11	0.0	1	2	Gabbro	33	0	2			Buff		0	1	1	0	0		2,6,12		0.1	1	
5	921C	1	1	2	13	16	0.1	1	2	Gabbro	28	0	2			Buff		0	1	1	0	0		2,6,12		0.1	1	
6	921C	1	1	3	29	5	0.3	1	2	Gabbro	33	0	2			Buff		0	1	1	0	0		2,6,12				
7	921C	2	1	1	0	11	10.0	2		Diabase	4	0	2			grey		0	1	1	0	0		5		1	2	0.5
8	921C	2	1	2	12	3	10.1	2		Diabase	0	0						0	0	0	0	0		0				
9	921C	2	1	3	16	7	10.2	2		Diabase	0	0						0	1	0	0	0		5				
10	921C	2	1	4	23	9	10.2	2		Diabase	0	0						0	1	0	0	0		5				
11	921C	2	1	5	34	6	10.3	3		Deformed gabbro	90	3				grey-green		0	0	0	0	0		0		1	3	0.5
12	921C	2	1	6	41	11	10.4	3		Altered deformed gabbro	90	3				grey-green		0	1	0	0	0		5		1	3	0.5
13	921C	2	1	7	53	4	10.5	3		Deformed gabbro	76	0	1			grey-green	UM	1	0	0	0	0		5		1	<1	
14	921C	2	1	8	57	12	10.6	3		Deformed gabbro	0	0						0	1	0	0	0		3,5				
15	921C	2	1	9	70	8	10.7	3		Deformed gabbro	0	0						0	0	0	1	4		0				
16	921C	2	1	10	79	10	10.8	3		Deformed gabbro	0	0						0	1	0	0	0		5				
17	921C	2	1	11	90	10	10.9	3		Deformed gabbro	0	0						0	0	0	0	0		3,5				
18	921C	2	1	12	102	2	11.0	3		Deformed gabbro	0	0						0	0	0	0	0		0				
19	921C	2	1	13	105	4	11.1	3		Deformed gabbro	0	0						0	1	0	0	0		5				
20	921C	2	1	14	110	15	11.1	3		Deformed gabbro	48	0				pale-green	UM	0	0	0	0	0		0				
21	921C	2	1	15	126	8	11.3	3		Deformed gabbro	15	0						0	1	0	0	0		3,5				
22	921C	2	1	16	135	4	11.3	3		Altered gabbro	0	0				grey		0	0	0	0	0		0				
23	921C	2	2	1	0	9	11.5	3	2	Gabbro	27	0	3			Grey		0	0	1	0	0	0	12				
24	921C	2	2	2	11	2	11.6	3	2	Gabbro	18	0	3			Greenish-grey		0	0	0	0	0		0				
25	921C	2	2	3	14	4	11.6	3	2	Gabbro	28	0	3			Slightly pinkish-grey		0	1	0	0	0		12				
26	921C	2	2	4	19	4	11.7	3	2	Gabbro	22	0	3			Slightly pinkish grey		0	1	0	0	0		12				
27	921C	2	2	5	24	8	11.7	4	2	Olivine gabbro	13	0		5		Slightly pinkish-grey		0	0	0	0	0		0		7		
28	921C	2	2	6	33	17	11.8	4	2	Olivine gabbro	3	0	2			Grey		0	0	0	0	0		0		8		
29	921C	2	2	7	51	31	12.0	4	2	Olivine gabbro	4	0	2			Grey		0	1	0	0	0		12		10		
30	921C	2	2	8	83	12	12.3	4	2	Olivine gabbro	4	0	2			Grey		0	1	0	0	0		12		15		

Figure 20. Example of VCD data recording template for Leg 153.

	AC	AD	AE	AF	AG	AH	AI	AJ	AK	AL	AM	AN	AO	AP	AQ	AR	AS	AT	AU	AV	AW	AX	AY	AZ	BA	BB	BC	BD	BE	BF	BG	
1																									MINERALOGY							
2	Crystal Shape	3D Crystal Shape	Preferred Orientation	Alteration	Cpx	Crystal size		Crystal Shape	3D Crystal Shape	Preferred Orientation	Alteration	Opx	Crystal size		Crystal Shape	3D Crystal Shape	Preferred Orientation	Alteration	Plag	Crystal size		Crystal Shape	3D Crystal Shape	Preferred Orientation	Alteration	Spinel	Other oxides	Sulfides	grain size, maximum	grain size, minimum	grain size, average	
3				(%)	(%)	max.	min.					(%)	(%)	max.	min.				(%)	(%)	max.	min.				(%)	%	%	y/n	(mm)	(mm)	
4	3	13		90	35	6		3	14		80								0	65	3		2	2		7		0.1	1	6	0	2
5	3	13		90	30	7		3	14		80									60	3		2	2		7		0.1	1	7	0	2
6					35	6		3	14		80									65	3		2	2		7		0.1	1	6	0	2
7	3	9		100																3	5	0.5	1	4		100			1			1
8																														0	0	
9																														0	0	
10																														0	0	
11	3	13		100	30	3	1	3	12		90									69	3	1	3	15		90			y			
12	3	13		100	30	3	1	3	12		90									69	3	1	3	15		90						
13	3	8		100	25	3	0.2	3	12		80									69	3	0.1	3	11		80						0
14																														0	0	
15																														0	0	
16																														0	0	
17																														0	0	
18																														0	0	
19																														0	0	
20					25	8	0.2	3	11		50									70	3	0.1	3	11		50					0	2
21					30	8	4	2	12		50																					
22																														0	0	3
23					42	3	1	3	13		30	1	4		2	3	13			57	3	1	2	4		25		1.0	y			2
24					40	8	1	2	4	0	30	1	4		2	3	13			59	6	1	2	4		10		1.0	y			3
25					40	6	1	2	4	0	40	2	4		2	3	13			59	6	1	2	4		20		1.0	y			3
26					40	4	1	2	4		40									59	4	1	2	4		10		1.0	y			2
27				40	38	8	1	3	13		20									54	10	1	2	4		5		1.0	y			3
28				20	35	4	1	3	13		5									56	5	1	2	4		0		1.0	y			2
29				20	35	7	1	3	13	0	5									54	8	1	2	4		0		1.0	y			3
30				20	25	4	1	3	13		5									59	3	1	2	4		0		1.0	y			2

Figure 20 (continued).

	BH
1	<b>ADDITIONAL COMMENTS</b>
2	
3	
4	Pieces 1 to 3 are all similar. Plag and cpx appear to have similar grain size but intergrowth features suggest that cpx is oikocrystic (up to 6mm). Cpx colour is very variable; from pearly pink-grey to brown and green. Alteration to amphiboles?
5	All three pices in this section are cut by pale kharky-green felted actinolite zones/veins. They are generally 3 - 5 mm wide (but occ. up tp 10 mm) and enclose lenses of equant cpx and plag grains, suggesting that they may be shear zones.
6	A vitreous green mineral lacking cleavage occurs interstitially, chiefly between plagioclase grains.
7	Porphyritic diabase,olivine is completly altered to chlorite and pyrite, plagioclase phenocrysts are altered to secondary plagioclase and chlorite. The groundmass is intergranular plagioclase (70%)+cpx(30%)+olivine (2%). Disseminated pyrite throughout.
8	
9	
10	
11	Strongly altered gabbro, olivine to chlorite, rare spots of pyrite.
12	
13	
14	Moderately altered foliated gabbro, rock strongly recrystallized,olivine to chlorite, cpx to brown amphibole and clay
15	Cut by chlorite-magnetite-sulphide zone. Cataclastic?
16	
17	
18	
19	
20	Very difficult rock, moderatly altered + chloritic veins. Texture may be cumulate containing intercumulate cpx.
21	
22	
23	Medium-grained gabbro cut by actinolite-chlorite vein 2-5mm thick, totally weathered under high oxidation conditions
24	Coarse-grained gabbro, some large pyroxene contained in patches with alteration of cpx to actinolite.
25	small fragment, clinopyroxene partly altered into chlorite
26	small fragment, clinopyroxene pervasively altered into chlorite and epidote
27	Coarse-grained gabbro, disseminated sulfides and opaque oxides.
28	Grain size of olivine gabbro,composed mostly of pl,cpx and ol, ranges from medium to coarse in the middle of the piece.
29	Contains 3 layers; 2 layer contacts; upper=med gr gabbro with high modal cpx; middle=c.g. gabbro w/ more plag; lower=similar to upper . Cut by thin vein (up to 2mm) of albite and chl. Green cpx rimmed by brown cpx.
30	Lithology is simmlar to the medium part of piece 7.

Figure 20 (continued).

Figure 21. Example of stand-alone structural data recording template (STRUC-LOG) for Leg 153.



Table 2. Terminology codes for Leg 153 linked spreadsheets (TERMINOL).

Rock names		Breccia clasts		Metamorphic facies		Igneous equigranular texture		Igneous inequigranular texture		Igneous cumulate texture	
Code	All forms	Code	MET_BREC	Code	MET_ROCK	Code	VCD, THINSEC.	Code	VCD, THINSEC.	Code	VCD, THINSEC.
1	Olivine gabbro (OGAB)	1	Serpentinite	1	Zeolite	0	If not equigranular	0	If not inequigranular	1	Orthocumulate (25%–50% trapped melt products)
2	Gabbro (GAB)	2	Gabbro	2	Greenschist	1	Panidiomorphic granular	1	Seriate	2	Mesocumulate (7%–25% trapped melt products)
3	Troctolite (TR)	3	Basalt	3	Greenschist-amphibolite	2	Hypidiomorphic granular	2	Poikilitic/oikocryst chadocrysts	3	Adcumulate (0%–7% trapped melt products)
4	Anorthosite (AN)	4	Peridotite	4	Amphibolite	3	Allotriomorphic granular	3	Intergranular	4	Heteradcumulates
5	Gabbronorite (GABN)	5	Breccia	5	Granulite	4	Aphyric	4	Ophitic	5	Crescumulate (elongate, skeletal, dendritic)
6	Norite (NOR)	6	Sandstone					5	Sub-ophitic		
7	Oxide gabbro (OXGAB)							6	Varitextured		
8	Oxide gabbronorite (OXGBN)							8	Pegmatitic		
9	Serpentinized lherzolite (LHZ)							9	Sparsely phyric (1%–2%)		
10	Serpentinized harzburgite (HRZ)							10	Moderately phyric (2%–10%)		
11	Serpentinized dunite (DUN)							11	Highly phyric (>10%)		
12	Websterite (WBST)							12	Glomerophyritic		
13	Serpentinized wehrlite (WEHR)										
14	Serpentinized olivine clinopyroxenite (OLCPX)										
15	Clinopyroxenite (CPX)										
16	Serpentinized olivine orthopyroxenite (OLOPX)										
17	Serpentinized olivine websterite (OLWBST)										
18	Orthopyroxenite (OPX)										
19	Chromitite (CHR)										
20	Serpentinite (SERP)										
21	Rodingite (ROD)										
22	Talc schist (TLCSCH)										
23	Diorite (DIOR)										
24	Quartz diorite (QTZDIOR)										
25	Tonalite (TON)										
26	Trondhjemite (TROND)										
27	Gabbroic pegmatite (GABPEG)										
28	Troctolitic pegmatite (TRPEG)										
29	Hbl-pl pegmatite (HBLPEG)										
30	Metagabbro (static>80% alt.)(METGAB)										
31	Gneissic gabbro (GNGAB)										
32	Mylonitic gabbro (MYLGAB)										
33	Amphibolite (AMPH)										
34	Diabase (DIAB)										
35	Porphyritic diabase (PRPHDIAB)										
36	Greenstone (GRNST)										
37	Glassy aphyric basalt (GLBAS)										
38	Aphyric basalt (APHBAS)										
39	Porphyritic basalt (PRPHBAS)										
40	Polygenic gravel										
41	Gravel										



Table 2 (continued).

Deformation intensity	Partitioning of deformation (ductile structures)		Minerals		Grain shape	3D shape		Preferred orientation		Zoning			
(Ductile structures)	Code	VCD	Code	Mineral abbrev.	Code	VCD, thinsec.	Code	VCD	Code	VCD	Code	T.S.	
Sum of deformation intensities from all ductile structures	0	No ductile structures	1	Actinolite	act	1	Euhedral	1	Equant	0	None	0	No Zoning
	1	Localized	2	Albite	ab	2	Subhedral	2	Tabular	1	Magmatic	2	Weak Zoning (thin rim)
	2	Penetrative	3	Antigorite	anti	3	Anhedral	3	Platy	2	Tectonite	3	Moderate Zoning
	*Decision is made based on scale of the observations (e.g., the piece scale, the thin section scale, the unit scale), and the response need not to be identical on each spreadsheet or form where there are different scales of observation. For example, on a thin-section form (microscopic) the deformation may be penetrative, on the VCD (macroscopic) the deformation may also be penetrative, but on the unit scale the deformation may be localized.		4	Apatite	ap	4	Lath	4	Lath			4	Strong Zoning (thick rim)
			5	Biotite	bi	5	Needle	5	Needle				
			6	Brown amphibole	B.am	6	Skeletal	6	Skeletal				
			7	Brucite	br	7	Octahedral	7	Octahedral				
			8	Carbonate	cc	8	Rounded	8	Rounded				
			9	Chalcopyrite	cpy	9	Globular	9	Globular				
			10	Chlorite	chl	10	Spheroidal	10	Spheroidal				
			11	Chrysotile	chry	11	Semi-rounded	11	Semi-rounded				
			12	Clay	cly	12	Sub-angular	12	Sub-angular				
			13	Clinopyroxene	cpx	13	Irregular	13	Irregular				
			14	Cummingtonite	cum	14	Jagged	14	Jagged				
			15	Epidote	ep	15	Elongate	15	Elongate				
			16	Hematite	hm	16	Spongy	16	Spongy				
			17	Hornblende	hbl	17	Holly leaf (sp)	17	Holly leaf (sp)				
			18	Hydro. diopside	H.cpx								
			19	Hydro. garnet	H.gar								
			20	Iddingsite	idd								
			21	Ilmenite	ilm								
			22	Iron oxide	feox								
			23	Lizardite	liz								
			24	Magnetite	mt								
			25	Native copper	Cu								
			26	Olivine	ol								
			27	Orthopyroxene	opx								
			28	Penlandite									
			29	Plagioclase	plg								
			30	Prehnite	pr								
			31	Pumpellyite	pmp								
			32	Pyrite	py								
			33	Pyrrhotite	pyh								
			34	Quartz	qtz								
			35	Secondary plagioclase	S.pl								
			36	Serpentine	ser								
			37	Silica	sio2								
			38	Smectite	smt								
			39	Sphalerite	sph								
			40	Spinel	sp								
			41	Talc	tlc								
			42	Titanite	tt								
			43	Titanomagnetite									
			44	Tremolite	trem								
			45	Zeolite	zeo								
			46	Zircon	zir								

Table 2 (continued).

Exsolution		Fluid inclusions		Mineral inclusions	General		Contacts		Other igneous textural comments (if necessary; can note more than one)		
Code	T.S.	Code	T.S.	T.S.	Code	???	Code	VCD	Code	VCD	Measurement of grain size and range
0	None	0	none	X within Y	0	no	1	Irregular intrusive	1	Weakly vesicular	Grain size is measured along the longest dimension of each mineral, and the maximum and minimum lengths measured for each primary mineral phases are recorded. In practice, this will include parts of the hydrous alteration phases that is known to replace the primary mineral grain. In the case of serpentinized olivine, the grain sizes can only be measured in thin Trachytic section by carefully reconstructing grain dimensions using Skeletal Crystalloptic continuity across the serpentine network by noting Perlitic similar extinction directions.
1	Blebs	1	liquid	e.g. Ol w/i CPX	1	yes	2	Cumulate	2	Moderately vesicular	
2	Thin Lamellae	2	brine				3	Fault	3	Scoriaceous	
3	Thick Lamellae	3	CO <sub>2</sub>				4	Shear zone	4	Pumaceous	
		4	methane				5	Grain size	5	Amygdaloidal	
		5	vapor				6	Textural changes	6	Miarolitic	
							7	Modal changes	7	Symplectic	
							8	Dike contact	8		
							9	Sill contact	9		
							10	Sharp	10		
							11	Gradational	11	Spherulitic	
									12	Variolitic	
									13	Microlitic	
									14	Intersertal	

Note: T.S. = thin section.